

Chapter one

Introduction

1-1 Introduction:

Ultrasound examination of the fetus became integrated into prenatal care (especially for measurement of fetal limb) soon after its introduction in the late 1950's. The past four decades have seen further improvements in ultrasound technology and advances in its utility as well as promotion of respect for patient's autonomy and involvement in medical care (Kurjak and Chervenak, 2003).

Ultrasound imaging is relatively inexpensive, safe, real-time, and readily available in hospitals and clinics throughout the world (Lazebnik, 2008).

Ultrasound has become one of primary tools used to evaluate the developing fetus during pregnancy. Obstetric ultrasound assess the development, growth, and wellbeing of the fetus (Hagen-Ansert, 2001).

Fetal growth is a result of complex interaction between several maternal, fetal and placental mechanisms. A final classification of neonatal growth outcome depends on how this development is defined. Most obstetricians rely on uterine fundal height, fetal abdominal circumference (AC) measurement and/ or a sonographic estimate of fetal weight for the detection of intrauterine growth restriction (IUGR). Fractional limb volume can be used for fetal growth assessment and weight estimation using three-dimensional ultrasonography (3DUS) (Lee et al.,2009).

Accurate assessment of gestational age is fundamental in managing both low and high risk pregnancies and may also assist obstetricians in appropriately counseling women who are at imminent risk of a preterm delivery about likely neonatal outcomes. Precise knowledge of gestational age is also essential in the evaluation of fetal growth and detection of intra-uterine growth restriction (Kurjak and Chervenak, 2003).

The use of multiple parameters (eg. BPD, HC, AC, FL) improved the accuracy of gestational age assessment compared with any single parameter. If the gestational age estimates derived from all of the parameters are similar, assignment of gestational age from the average of all the parameters will improve accuracy (JainA et al.,2001).

All ultrasound examinations benefit from amethodical approach and this is especially true when measurements are required. In addition, the comparative interpretation of various measurements are all important pointers to potential problems (Chudleigh and Thilaganathan, 2004).

Sonographic measurement of the ossified shafts of fetal long bones is possible after 12th week of gestational age (Exacoustos et al., 1991).

Measurement of fetal limbs can be used to date pregnancies as well as forming an important part of the assessment of fetal anatomy. The femur length is the most commonly used limb measurement and is usually included as a routine part of any fetal anomaly scan. However, when signs indicating the possibility of a skeletal dysplasia are found, more extensive evaluation of all long bones is needed to aid diagnosis (Chitty and Altman,2002).

Several studies have established standard growth curves for the femur, but only a few authors have described normal values of the tibia, fibula, radius, and ulna (Robinson, 1995).

Use of lengths of two or more bones in predicting gestational age is necessary and mean gestational age obtained from such combinations is preferred (Jeanty P et al, 1984).

Currently, the sonographic estimation is derived from calculations based on fetal measurements and serves as an indirect indicator of gestational age. (Kurjak and Chervenak, 2003).

1-2 Objectives:

1-2-1 General objective:

To measure fetal radius, ulna, fibula and tibia lengths of normal singleton pregnant Sudanese women between 14th and 38th weeks by using ultrasound.

1-2-2 Specific objective:

1. To assess the relation between ultrasonic measurement of fetal radius and gestational age at 14, 18, 22, 26, 30, 34, 38 weeks.
2. To assess the relation between ultrasonic measurement of fetal ulna and gestational age at 14, 18, 22, 26, 30, 34, 38 weeks.
3. To assess the relation between ultrasonic measurement of fetal fibula and gestational age at 14, 18, 22, 26, 30, 34, 38 weeks.
4. To assess the relation between ultrasonic measurement of fetal tibia and gestational age at 14, 18, 22, 26, 30, 34, 38 weeks.

1-3 Problem of study:

No more studies have established the growth patterns of fetal radius, ulna, fibula and tibia in normal Sudanese pregnant women. So this study is an attempt to measure fetal radius, ulna, fibula and tibia lengths.

1-4 Thesis outline:

This study will be built in five chapters. Chapter one will deal with introduction, objectives, problem of the study, and thesis outline. Chapter two will highlight the literature review. Chapter three will express the methodology of the study. Chapter four will include the presentation of results. Chapter five will concern with the discussion, conclusion, and recommendations.

Chapter two

Literature review

2-1 Fetal anatomy and embryology:

2-1-1 First week of development (ovulation to Implantation):

With each ovarian cycle, a number of primary follicles begin to grow, but usually only one reaches full maturity, and only one oocyte is discharged at ovulation. At ovulation, the oocyte is in metaphase of the second meiotic division and is surrounded by the zona pellucida and some granulosa cells (Fig.2.1). Sweeping action of tubal fimbriae carries the oocyte into the uterine tube (Salder, 2015).

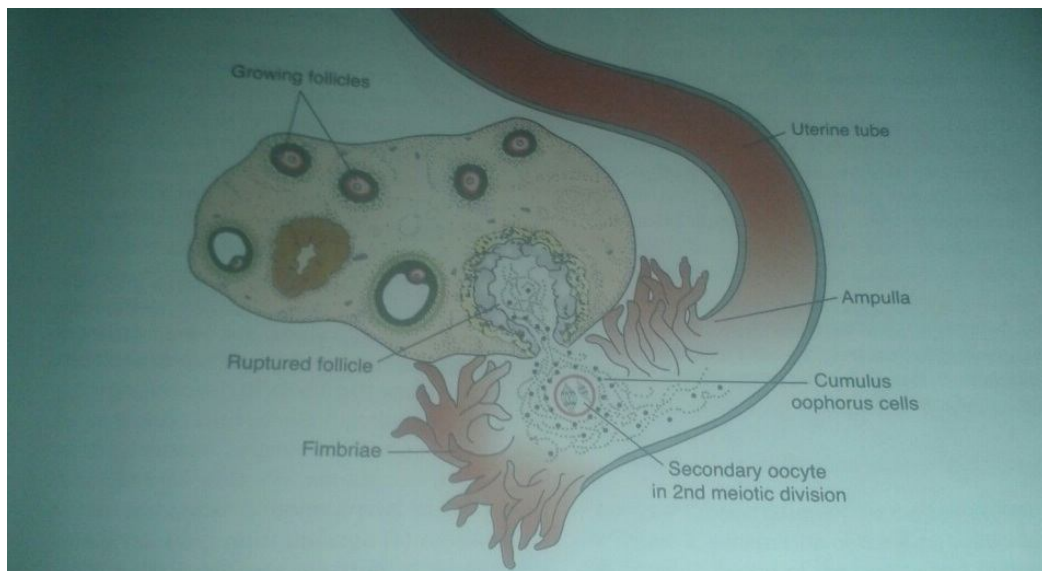


Figure (2.1) diagram shows Relation of fimbriae and ovary. Fimbriae collect the oocyte and the uterine tube (Salder,2015).

As soon as the spermatozoa has entered the oocyte: oocytes finishes its second meiotic division and forms the female pronucleus, the zona pellucida becomes impenetrable to other spermatozoa, the head of the sperm separates from the tail, swells, and forms the male pronucleus (Fig. 2.2 and 2.3) (Salder, 2015).

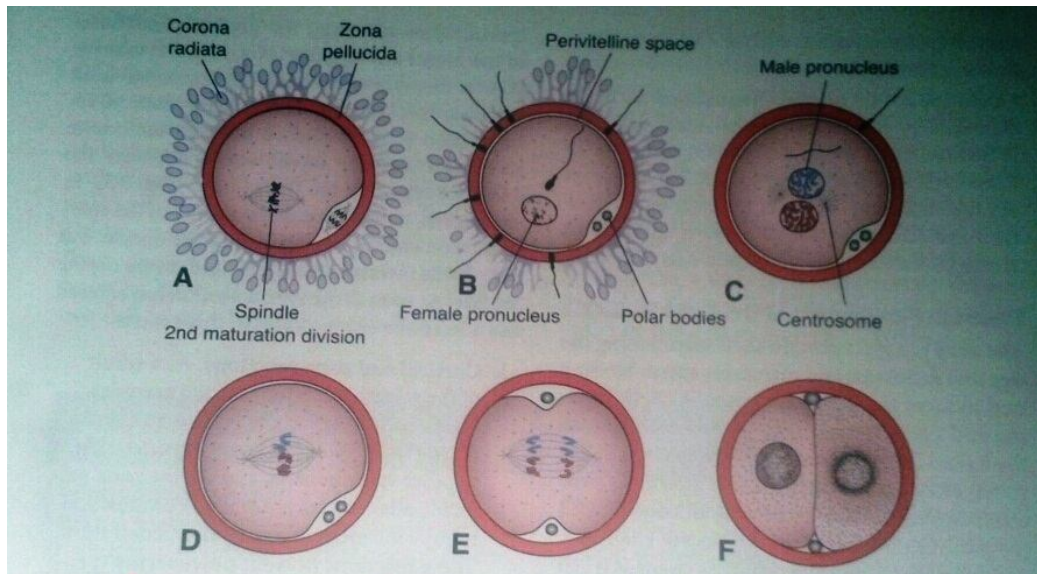


Figure (2.2) diagram illustrates A, Oocyte immediately after ovulation, showing the spindle of the second meiotic division. B, Aspermatozoon has penetrated the oocyte, which has finished its second meiotic division. Chromosomes of the oocyte are arranged in a vesicular nucleus, the female pronucleus. Heads of several sperm are stuck in the zona pellucid. C. Male and female pronuclei. D,E. Chromosomes become arranged on the spindle, split longitudinally, and move to opposite poles. F. Two-cell stage (Salder, 2015).

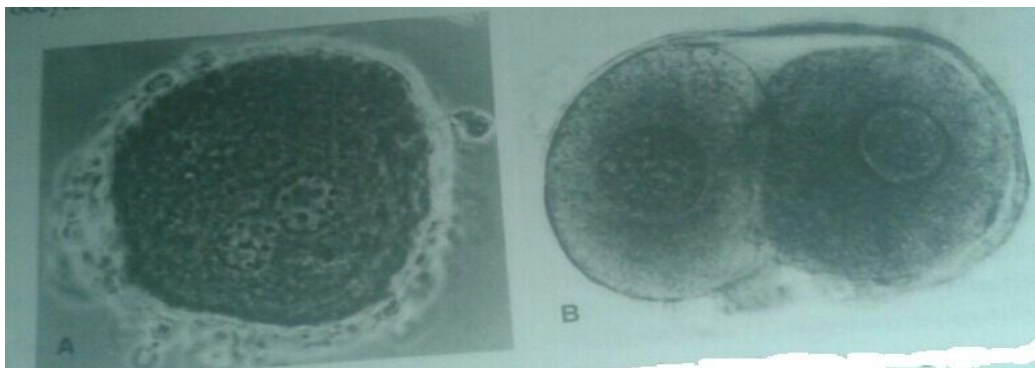


Figure (2.3) diagram shows A, Phase contrast view of the pronuclear stage of a fertilized human oocyte with male and female pronuclei. B, Two-cell stage of human zygote (Salder,2015).

After both pronuclei have replicated their DNA, paternal and maternal chromosomes intermingle, split longitudinally, and go through ameiotic

division, giving rise to the two-cell stage. The results of fertilization are restoration of the diploid number of chromosomes determination of chromosomal sex, initiation of cleavage. Cleavage is a series of mitotic divisions that results in an increase in cells, blastomeres, which become smaller with each division. After three divisions, blastomeres undergo compaction to become a tightly grouped ball of cells with inner and outer layers. Compacted blastomeres divide to form a 16-cell morula. As the morula enters the uterus on the third or fourth day after fertilization, a cavity begins to appear, and the blastocyst forms. The inner cell mass, which is formed at the time of compaction and will develop into the embryo proper, is at one pole of the blastocyst. The outer cell mass, which surrounds the inner cell and the blastocyst cavity, will form the trophoblast. The uterus at the time of implantation is in secretory phase, and the blastocyst implants in the endometrium along the anterior or posterior wall (Fig. 2.4) (Salder,2015).

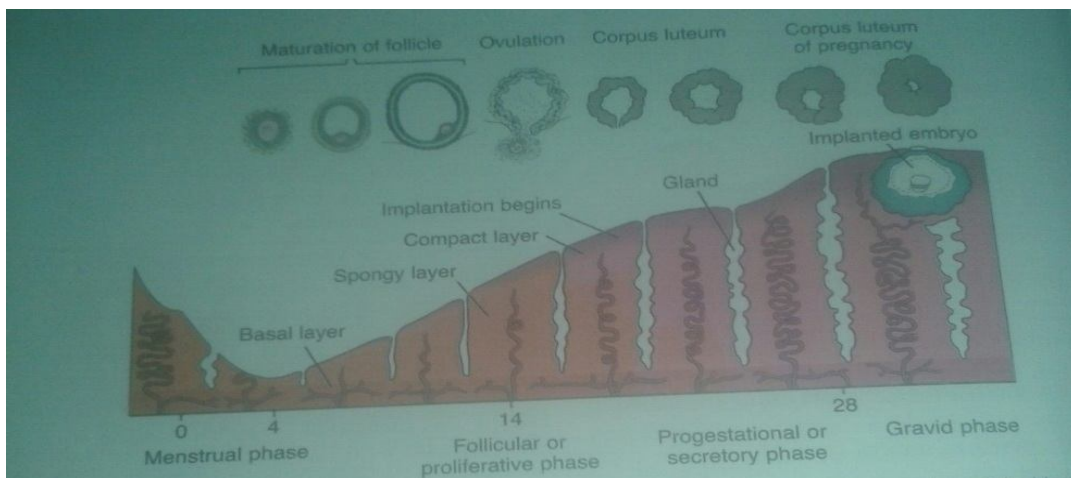


Figure (2.4) diagram illustrates changes in the uterine mucosa correlated with those in the ovary. Implantation of the oocyte has caused development of a large corpus luteum of pregnancy. Secretory activity of the endometrium increases gradually as a result of large amounts of progesterone produced by the corpus luteum of pregnancy (Salder, 2015).

2-1-2 Second week of Development(Bilaminar Germ Disc):

At the beginning of the second week, the blastocyst is partially embedded in the endometrial stroma. The trophoblast differentiates into an inner, actively proliferating layer, the cytotrophoblast; and an outer layer, the syncytiotrophoblast, which erodes maternal tissues (fig. 2.5). By day 9, lacunae develop in the syncytiotrophoblast. Subsequently, maternal sinusoids are eroded by the syncytiotrophoblast, maternal blood enters the lacunar network, and by the end of the second week, a primitive uteroplacental circulation begins (Fig. 2.5). The cytotrophoblast, meanwhile, forms cellular columns penetrating into and surrounded by the syncytium. These columns are primary villi. By the end of the second week, the blastocyst is completely embedded, and the surface defect in the mucosa has healed (Fig. 2.5) (Salder, 2015).

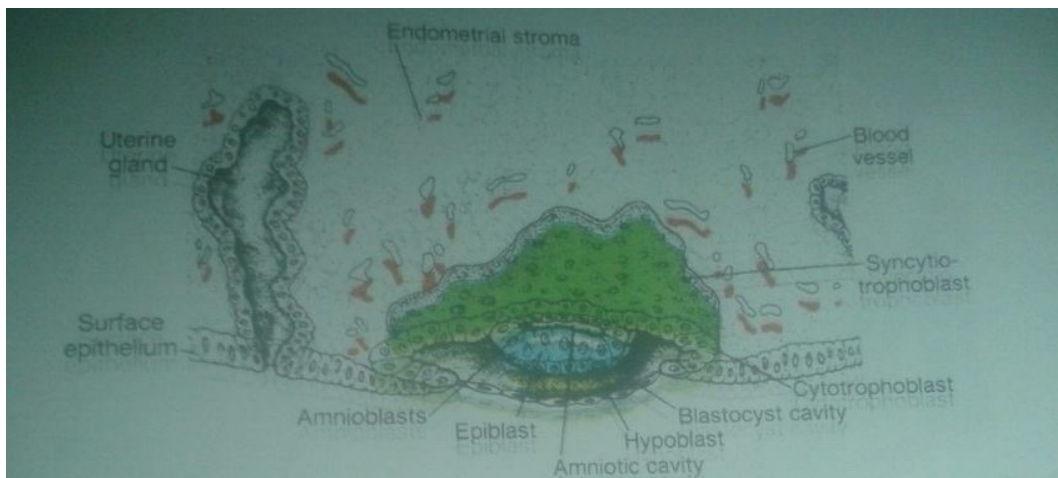


Figure (2.5) diagram shows A 7.5-day human blastocyst, partially embedded in the endometrial stroma. The trophoblast consist of an inner layer with mononuclear cells, the cytotrophoblast, and an outer without distinct cell boundaries, the syncytiotrophoblast. The embryoblast is formed by the epiblast and hypoblast layers. The amniotic cavity appears as small cleft (Salder, 2015).

The inner cell mass or embryoblast, meanwhile, differentiates into the epiblast and the hypoblast, together forming a bilaminar disc (Fig. 2.7).

Epiblast cells give rise to amnioblasts that line the amniotic cavity superior to the epiblast layer. Hypoblast cells are continuous with the exocoelomic membrane, and together they surround the primitive yolk sac (Fig. 2.6). By the end of the second week, extraembryonic mesoderm fills the space between the trophoblast and the amnion and exocoelomic membrane internally. When vacuoles develop in this tissue, the extraembryonic coelom or chorionic cavity forms (fig.2.7). Extraembryonic mesoderm lining the cytotrophoblast and an amnion is extraembryonic somatic mesoderm; the lining surrounding the yolk sac is extraembryonic splanchnic mesoderm (Fig.2.7) (Sadler, 2015).

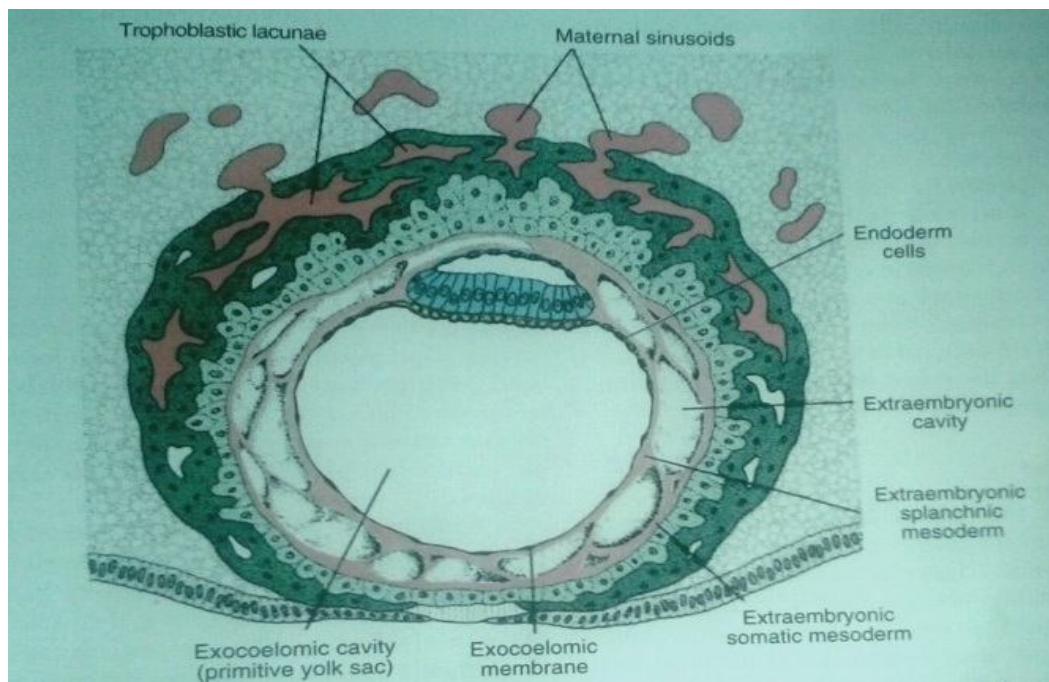


Figure (2.6) diagram shows human blastocyst of approximately 12 days. The trophoblastic lacunae at the embryonic pole are in open connection with maternal sinusoids in the endometrial stroma. Extraembryonic mesoderm proliferates and fills the space between the exocoelomic membrane and the inner aspect of the trophoblast (Salder, 2015).

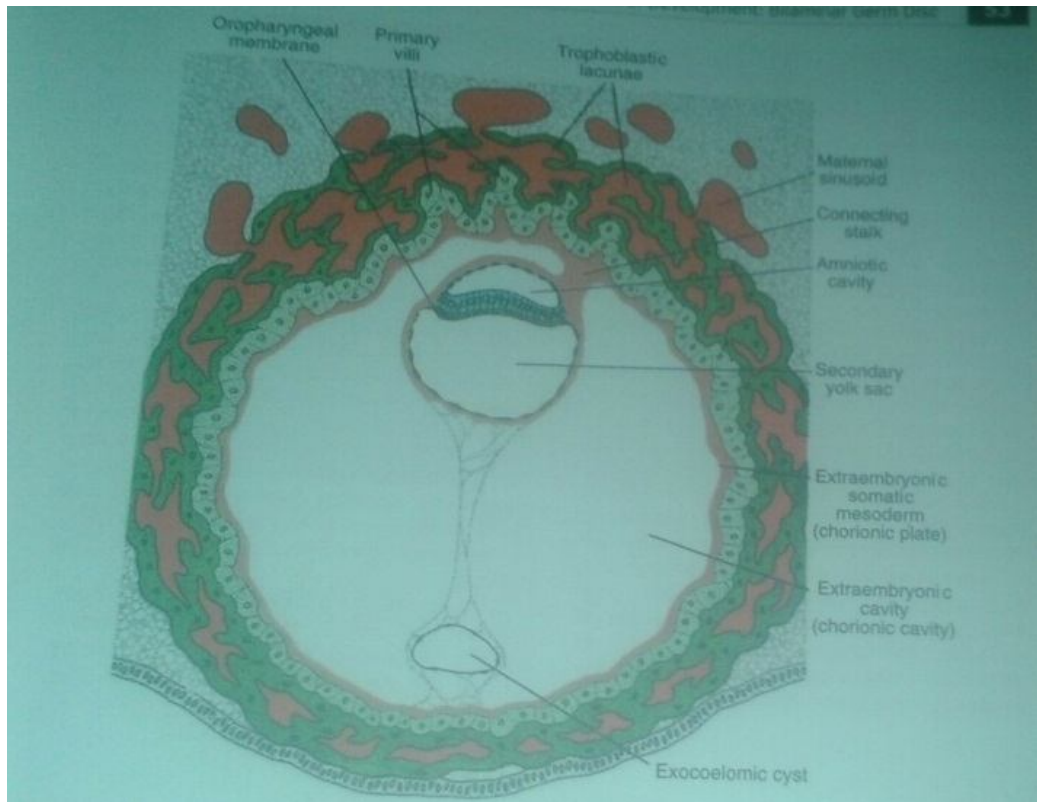


Figure (2.7) diagram shows A, 13-day human blastocyst. Trophoblastic lacunae are present at the embryonic as well as the embryonic pole, and the uteroplacental circulation has begun. Note the primary villi and the extraembryonic coelom or chorionic cavity. The secondary yolk sac is entirely lined with endoderm (Salder, 2015).

The second week of development is known as (the week of 2's) because the trophoblast differentiates into 2 layers, the cytotrophoblast and syncytiotrophoblast; the embryo blast forms 2 layers, the epiblast and hypoblast; the extraembryonic mesoderm splits into 2 layers, the somatic and splanchnic layers; two cavities form: the amniotic and yolk sac cavities (Sadler, 2015).

2-1-3 Third to Eighth weeks(the embryonic period):

The embryonic period, which extends from the third to the eighth weeks of development, is the period during which each of the three germ layers, ectoderm, mesoderm, and endoderm, gives rise to its own tissues and organ systems. As a result of organ formation, major features of body form are

established. The ectodermal germ layer gives rise to the organs and structures that maintain contact with the outside world are Central nervous system, Peripheral nervous system, Sensory epithelium of ear, nose, and eye, Skin, including hair and nails, Pituitary, mammary, and sweat glands and enamel of the teeth. Important components of the mesodermal germ layer are paraxial, intermediate, and lateral plate mesoderm. Paraxial mesoderm forms somitomeres, which give rise to mesenchyme of the head and organize into somites in occipital and caudal segments. Somites give rise to the myotome (muscle tissue), sclerotome (cartilage and bone), and dermatome (dermis of skin), which are all supporting tissues of the body (Sadler, 2015).

The vertebral column and ribs arise from somites, and the limbs arise from the lateral plate mesoderm. Limb development begins the 26th or the 27th day after conception with the appearance of upper limb buds. Lower extremity development begins 2 days later. Although the stages of development for the upper and lower extremities are the same, lower extremity development continues to lag behind that of the upper extremities (Hagen-Ansert, 2001).

Mesoderm also gives rise to the vascular system (i.e., the heart, arteries, veins, lymph vessels, and all blood and lymph cells). Furthermore, it gives rise to the urogenital system: kidneys, gonads, and their ducts (but not the bladder). Finally, the spleen and cortex of the suprarenal glands are mesodermal derivatives. The endodermal germ layer provides the epithelial lining of the gastrointestinal tract, respiratory tract, and urinary bladder. It also forms the parenchyma of the thyroid, parathyroids, liver, and pancreas. Finally, the epithelial lining of the tympanic cavity and auditory tube originates in the endodermal germ layer. As a result of formation of organ systems and rapid growth of the central nervous system, the initial flat embryonic disc begins to lengthen and to form head and tail regions (folds) that cause the embryo to curve into fetal position. the embryo also forms two

lateral body wall folds that grow ventrally and close the ventral body wall. As a result of this growth and folding, the amnion is pulled ventrally and the embryo lies within the amniotic fluid (Fig. 2.8). Connection with the yolk sac and placenta is maintained through the vitelline duct and umbilical cord, respectively (Salder, 2015).

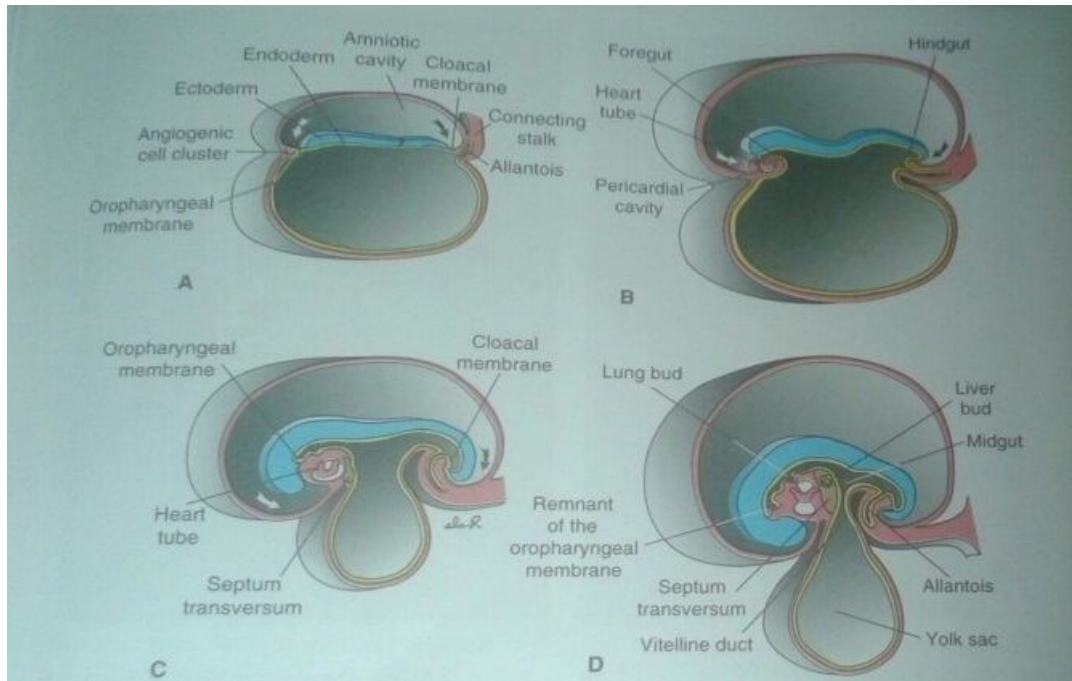


Figure (2.8) diagram shows sagittal midline sections of embryos at various stages of development to demonstrate cephalocaudal folding and its effect on position of the endoderm-linked cavity. A, 17 days. B, 22days. C,24 days. D, 28 days. Arrows, head and tail (Salder, 2015).

At the end of the third week, the neural tube is elevating and closing dorsally while the gut tube is rolling and closing ventrally to create a "tube on top of tube." Mesoderm holds the tubes together and the lateral plate mesoderm splits to form a visceral (splanchnic) layer associated with gut and a parietal (somatic) layer that, together with overlying ectoderm, forms the lateral body wall folds. the space between the visceral and parietal layers of lateral plate mesoderm is the primitive body cavity (Fig. 2.9). when the lateral body wall folds move ventrally and fuse in the midline, the body cavity is closed,

except in the region of the connecting stalk (Fig. 2.9 and 2.10). Here the gut tube maintains an attachment to the yolk sac as the yolk sac (vitelline) duct. The lateral body wall folds also pull the amnion with them so that the amnion surrounds the embryo and extends over the connecting stalk, which becomes the umbilical cord (Fig.2.9D and 2.10D) (Salder, 2015).

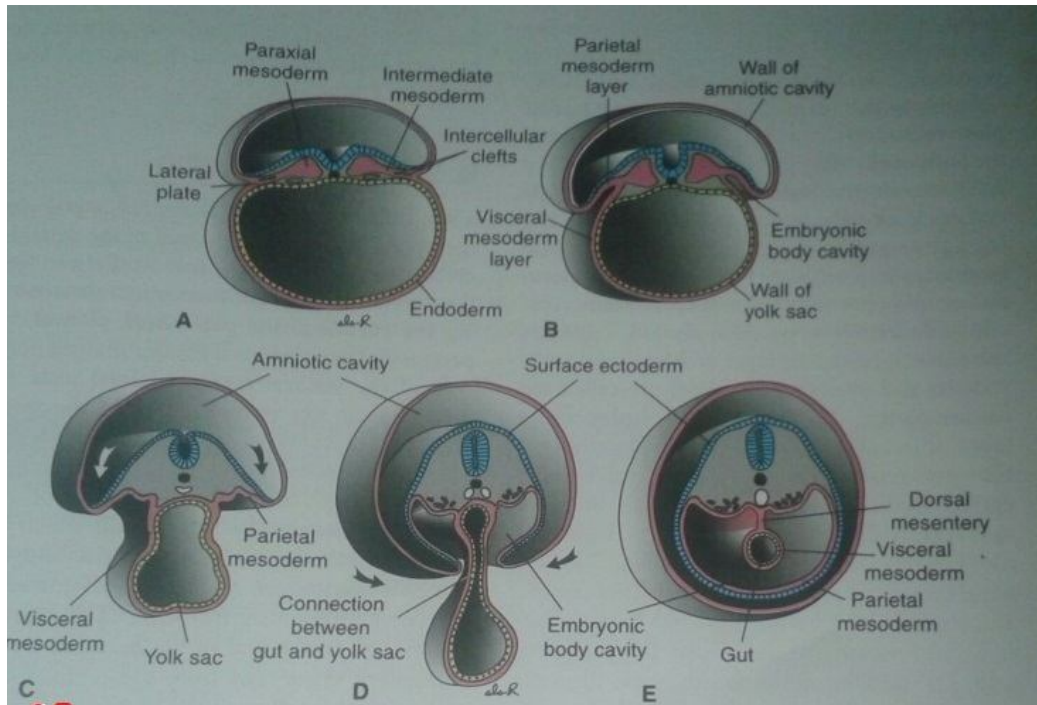


Figure (2.9) diagram shows transverse sections through embryos at various stages of the closure of the gut tube and ventral body wall. A, At approximately 19 days, intercellular cells are visible in the lateral plate mesoderm. B, At 20 days, the lateral plate is divided into somatic and visceral mesoderm layers that line the primitive body cavity (intraembryonic cavity). C, By 21 days, the primitive body cavity (intraembryonic cavity) is still in open communication with extraembryonic cavity. D, By 24 days, the lateral body wall folds, consisting of the parietal layer of the lateral plate mesoderm and overlying ectoderm are approaching each other in the midline. E, At the end of the fourth week, visceral mesoderm layers are continuous with parietal layers as a double-layered membrane, the dorsal

membrane, the dorsal mesentery. Dorsal mesentery extends from the caudal limit of the foregut to the end of hind gut (Salder, 2015)

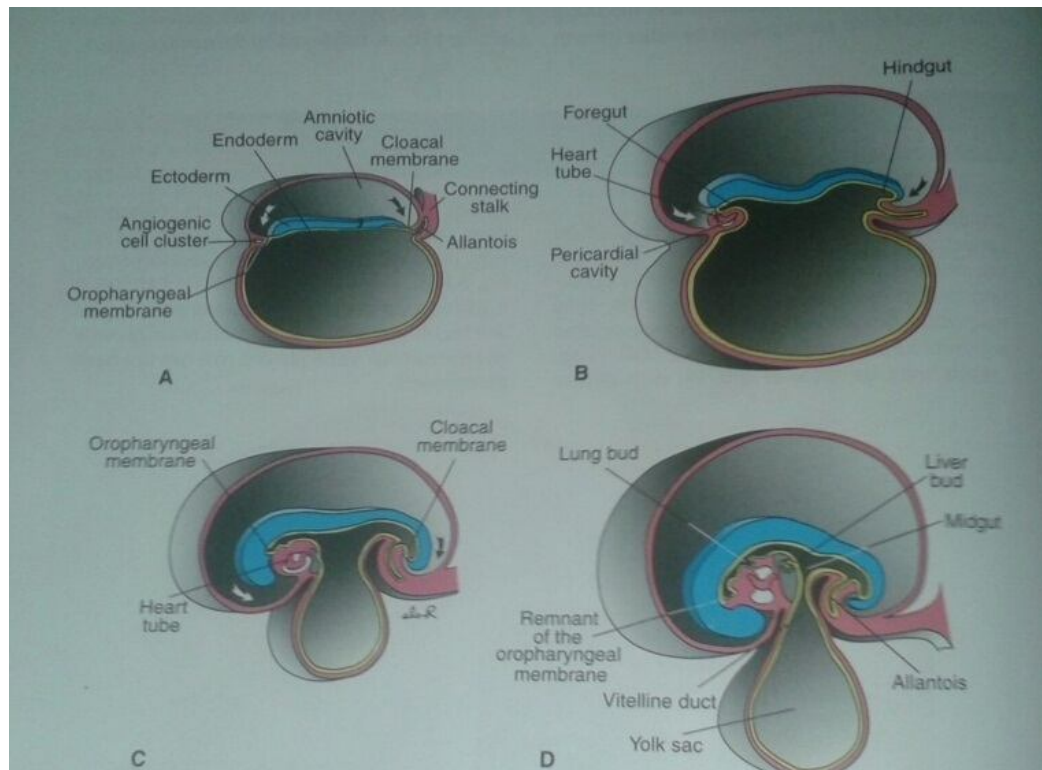


Figure (2.10) diagram shows midsagittal sections of embryos at various stages of development showing cephalocaudal folding and its effects upon position of the heart, septum transversum, yolk sac, and amnion. Note that, as folding progresses, the opening of the gut tube into the yolk sac narrows until it forms a thin connection, the vitelline (yolk sac) duct, between the midgut and yolk sac (D). Simultaneously, the amnion is pulled ventrally until the amniotic cavity nearly surrounds the embryo. A, 17 days. B, 22

days. C, 24 days. D, 28 days. Arrows, head and tail folds (Salder, 2015).

Parietal mesoderm will form the parietal layer of serous membranes lining the outside (walls) of the peritoneal, pleural, and pericardial cavities. The visceral layer of the serous membranes covering the lungs, heart, and abdominal organs. These layers are continuous at the root of each organ as the organs lie in their respective cavities. In the gut, the layers form the peritoneum places suspend the gut from the body wall as double layers of

peritoneum called mesenteries (Fig.2.9E). Mesenteries provide a path way for vessels, nerves, and lymphatics to the organs. Initially, the gut tube from the caudal end of the foregut to the end of the hindgut is suspended from the dorsal body wall by dorsal mesentery (Fig. 2.9E). Ventral mesentery, derived from the septum transversum, exists only in the region of the terminal part of the esophagus, the stomach, and the upper portion of the duodenum. The diaphragm divides the body cavity into the thoracic and peritoneal cavities. It develops from four components: septum transversum (central tendon), pleuroperitoneal somites at cervical levels three to five (C3-5) of the body wall (Fig. 2.11). Because the septum transversum is located initially opposite cervical segments three to five and because muscle cells for the diaphragm originate from somites at these segments, the phrenic nerve also arises from these segments of the spinal cord (C3, C4, and C5 keep the diaphragm alive) (Salder,2015).

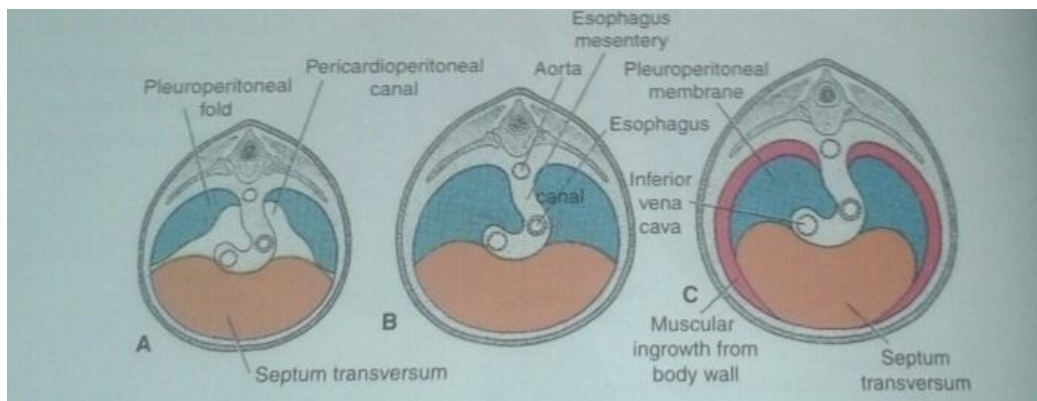


Figure (2.11) diagram illustrates development of the diaphragm. A. Pleuroperitoneal folds appear at the beginning of the fifth week. B. Pleuroperitoneal folds fuse with septum transversum and mesentery of the esophagus in the seventh week, separating the thoracic cavity from the abdominal cavity. C. Transverse section at the fourth month of development. An additional rim derived from the body wall forms the most peripheral part of the diaphragm (Salder, 2015).

The thoracic cavity is divided into the pericardial cavity and two pleural cavities for the lungs by the pleuropericardial membranes (Fig. 2.12) (Salder, 2015).

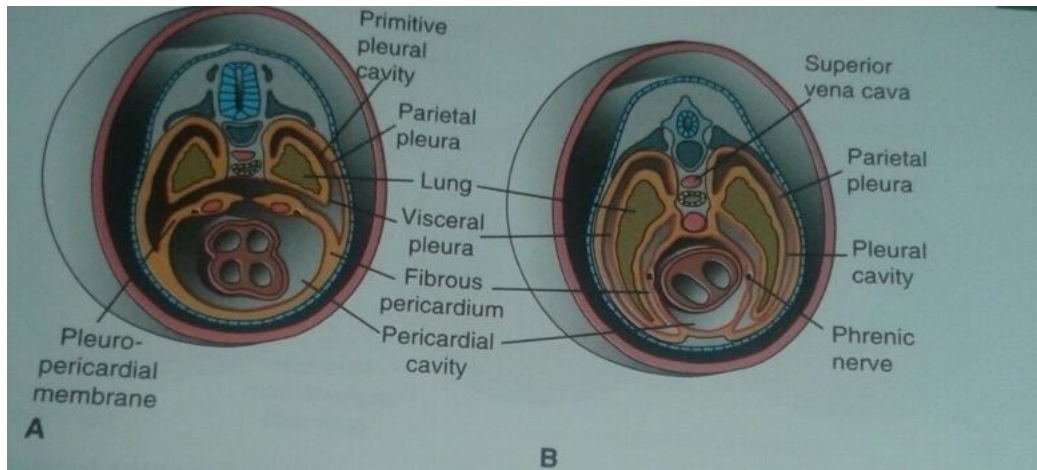


Figure (2.12) diagram shows A. Transformation of the pericardioperitoneal canals into the pleural cavities and formation of the pleuropericardial membranes. Note the pleuropericardial folds containing the common cardinal vein and phrenic nerve. Mesenchyme of the body wall forms the pleuropericardial membranes and definitive body wall. B. The thorax after fusion of the pleuropericardial folds with each other and with the root of the lungs. Note the position of the phrenic nerve, now in the fibrous pericardium. The right common cardinal vein has developed into the superior vena cava (Salder, 2015).

2-1-4 Third Month to Birth: The fetus and placenta:

The fetal period extends from the ninth week of gestation until birth and is characterized by rapid growth of the body and maturation of organ systems. Growth in length is particularly striking during the third, fourth, and fifth months (approximately 5cm per month), whereas increase in weight is most striking during the last 2 months of gestation (approximately 700 g per month). One of the most striking changes taking place during fetal life is the relative slow down in growth of the head compared with the rest of the body. At the beginning of the third month, the head constitutes approximately half

of the CRL. By the fifth month, the size of the head is about one third of the CHL, and at birth, it is one quarter of the CHL (Figure 2.13) (Salder, 2015).

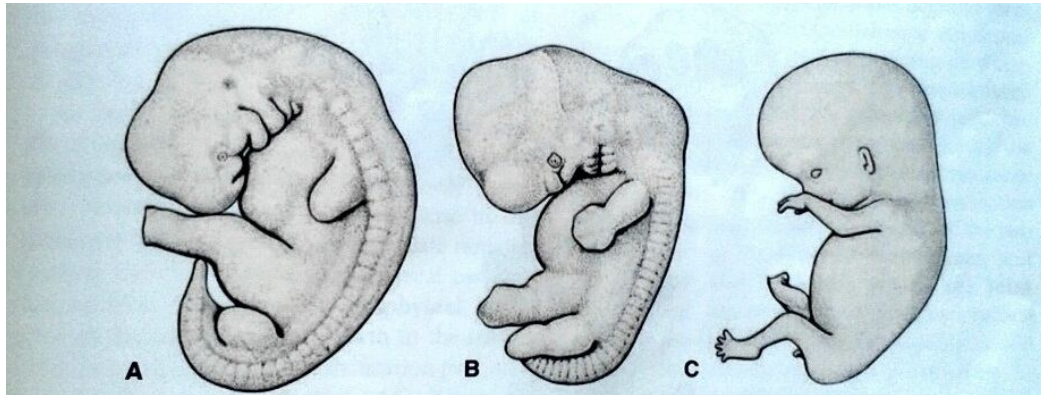


Figure (2.13) diagram shows size of the head in relation to the rest of the body at various stages of development (Salder, 2015).

During the third month, the face becomes more human looking. The eyes, initially directed laterally, move to ventral aspect of the face, and the ears come to lie close to their definitive position at the side of the head. The limbs reach their relative length in comparison with the rest of the body, although the lower limbs are still a little shorter and less well developed than the upper extremities. Primary ossification centers are present in the long bones and skull by the 12th week. Also by the 12th week, external genitalia develop to such degree that the sex of the fetus can be determined by external examination (ultrasound). During the sixth week, intestinal loops cause a large swelling (herniation) in the umbilical cord, but by 12th week, the loops have withdrawn into the abdominal cavity. At the end of the third month, reflex activity can be evoked in aborted fetus, indicating muscular activity. During the fifth month, fetal movements are clearly recognized by the mother, and the fetus is covered with fine, small hair. A fetus born during the sixth or the beginning of the seventh month has difficulty surviving, mainly because the respiratory and central nervous systems have not differentiated sufficiently. In general, the length of pregnancy for a full term fetus is considered to be 280 days, or 40 weeks after onset of the last

menstruation, or, more accurately, 266 days or 38 weeks after fertilization. The placenta consists of two components a fetal portion, derived from the chorion frondosum or villous chorion, and a maternal portion, derived from the decidua basalis. The space between the chorionic and decidua plates is filled with intervillous lakes of maternal blood. Villous trees (fetal tissue) grow into the maternal blood lakes and are bathed in them. The fetal circulation is at all times separated from the maternal circulation by a syncytial membrane (a chorion derivative) and endothelial cells from fetal capillaries. Hence, the human placenta is of the hemochorial type. Intervillous lakes of the fully grown placenta contain approximately 150 ml of maternal blood, which is renewed three or four times per minute. The villous area varies from 4 to 14 m², facilitating exchange between mother and child. Main functions of the placenta are exchange of gases; exchange nutrients antibodies, providing the fetus with passive immunity; production of hormones, such as progesterone, estradiol, and estrogen (in addition, it produces hCG and somatomammotropin); and detoxification of some drugs. The amnion is a large sac containing amniotic fluid in which the fetus is suspended by its umbilical cord. The fluid absorbs jolts, allows for fetal movement, and prevents adherence of the embryo to surrounding tissues. The fetus swallows amniotic fluid, which is absorbed through its gut and cleared by the placenta. The fetus adds urine to the amniotic fluid, but this is mostly water. The umbilical cord, surrounded by the amnion, contains two umbilical arteries, one umbilical vein, and (3) Wharton jelly, which serves as a protective cushion for the vessels (Salder, 2015).

2-1-5 Limb growth and development:

At the end of the fourth week of development, limb buds become visible as outpocketings from the ventrolateral body wall (Fig. 2.14A).

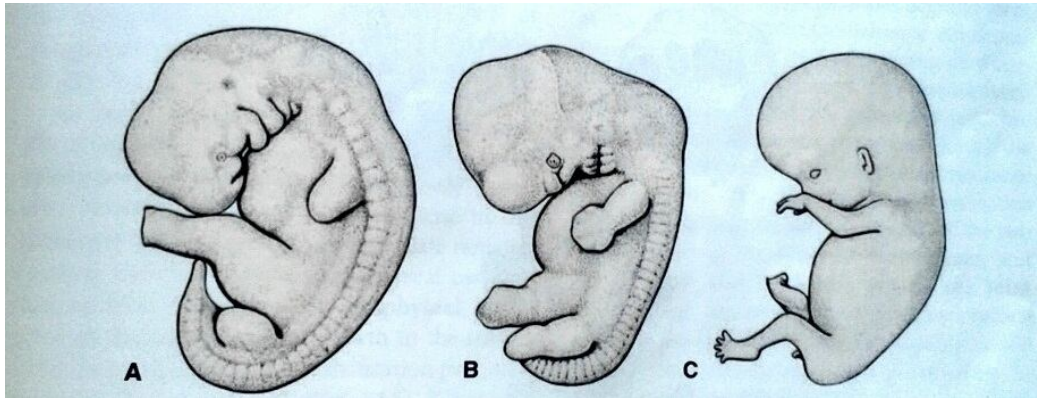


Figure (2.14) diagram illustrates development of the limb buds in human embryos. A. At 5 weeks. B. At 6 weeks. C. At 8 weeks. Hind limb development lags behind forelimb development by 1 to 2 days (Salder, 2015).

Limb buds along the body wall adjacent to specific spinal segments determined by HOX genes (upper limb buds lie opposite the lower cervical and upper two thoracic segment, and the lower limb buds lie opposite the lower four lumbar and upper two sacral segments). The AER at the distal border of the limb regulates proximodistal limb growth by secreting FGFS that maintain a region of rapidly dividing cells immediately adjacent to the ridge called the undifferentiated zone (Fig 2.15). As the limb grows, cells near the flank are exposed to retinoic acid that causes them to differentiate into the stylopod (humerus/femur). Next to differentiate is the zeugopod (radius/ulna and tibia/fibula), then the autopod (wrist and fingers, ankle and toes) (Salder, 2015).

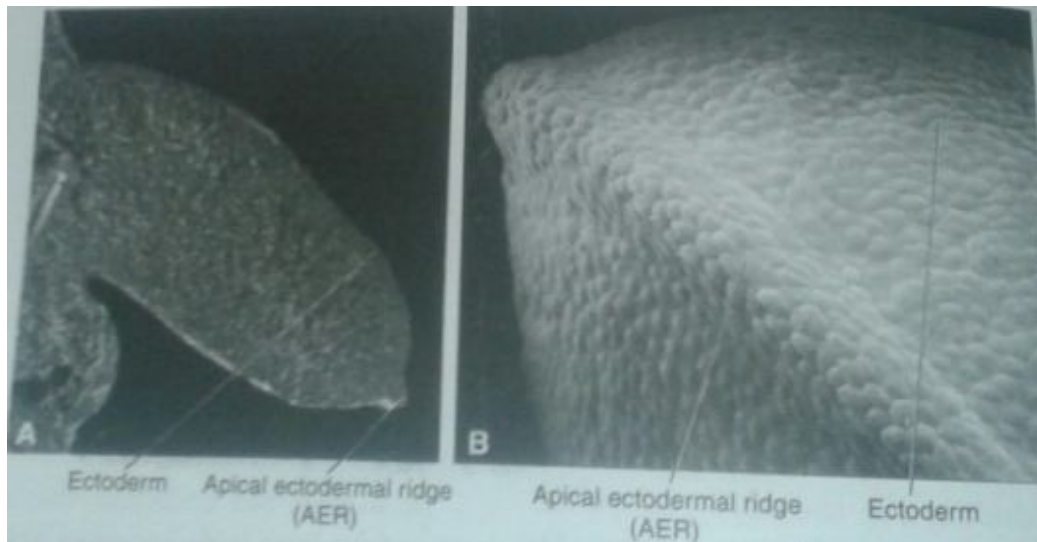
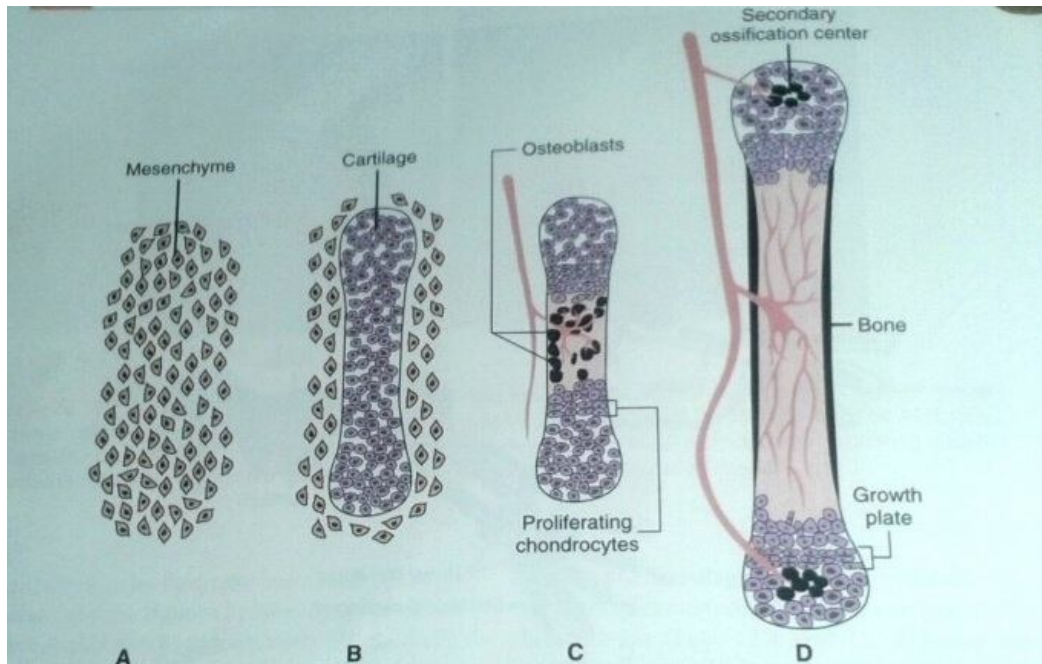


Figure (2.15) diagram shows A. Longitudinal section through the limb bud of a chick a core of mesenchyme covered by a layer of ectoderm that thickens at the distal border of the limb to form the AER. In human this occurs during the fifth week of development. B. External view of a chick limb at high magnification showing the ectoderm and the specialized region at the tip of the limb called the AER (Salder, 2015)

Ossification of the bones of the extremities, endochondral ossification, begins by the end of the embryonic period. Primary ossification centers are present in all long bones of the limbs by the 12week of development. From the primary center in the shaft or diaphysis of the bone, endochondral ossification gradually progresses toward the end of the cartilaginous model (Fig 2.16) (Salder,2015).



Figure(2.16) diagram illustrates endochondral bone formation. A. Mesenchyme cells begin to condense and differentiate into chondrocytes form a cartilaginous model of the prospective bone. C,D. Blood vessels invade the center of the cartilaginous model, bringing osteoblast (black cells) and restricting proliferating chondrocytic cells to the ends (epiphyses) of the bones. Chondrocytes toward the shaft side (diaphysis) undergo hypertrophy and apoptosis as they mineralize the surrounding matrix. Osteoblasts bind to the mineralized matrix and deposit bone matrices. Later, as blood vessels invade the epiphyses, secondary ossification centers form. Growth of the bones is maintained by proliferation of chondrocytes in the growth plates (Salder, 2015).

At birth, the diaphysis of the bone is usually completely ossified, but the two ends the epiphyses, are still cartilaginous. Shortly thereafter, however, ossification centers arise in the epiphyses. Temporarily, a cartilage plate remains between the diaphyseal and epiphyseal ossification centers. This plate, the epiphyseal plate, plays an important role in growth in the length of the bones. Endochondral ossification proceeds on both sides of the plate

(Fig.2.16). When the bone has acquired its full length, the epiphyseal plates disappear, and the epiphyses unite with the shaft of the bone. In long bones, an epiphyseal plate is found on each extremity; in smaller bones, such as the phalanges, it is found only at one extremity; and in irregular bones, such as the vertebrae, one or more primary centers of ossification and usually several secondary centers are present. Digits form apoptosis (programmed cell death) occurs in the AER to separate this structure into five separate ridges. Final separation of the digits is achieved by additional apoptosis in the interdigital spaces. Many digital defects occur that are related to these patterns of cell death, including polydactyly, syndactyly, and clefts (Salder, 2015).

2-2 Pathology

2-2-1 Anencephaly:

Anencephaly is the most common neural tube defect, with an overall incidence of approximately 1 in 1200 pregnancies. Anencephaly, which means absence of the brain, is caused by failure of closure of the neural tube at the cranial end. The result is absence of the cranial vault, complete or partial absence of the forebrain, which may partially develop and then degenerate, and the presence of the brain stem, midbrain, skull base, and facial structures. The remnant brain is covered by a thick membrane called angiomasous stroma or cerebrovasculosa (Hagen-Ansert, 2001).

2-2-2 Acrania:

Acrania is a lethal anomaly that manifests as absence of the cranial bones with the presence of complete, although abnormal, development of the cerebral hemispheres. This anomaly occurs at the beginning of the 4th gestational week when the mesenchymal tissue fails to migrate and does not allow bone formation over the cerebral tissue (Hagen-Ansert, 2001).

2-2-3 Cephalocele:

A cephalocele is a neural tube defect in which the meninges alone or meninges and brain herniated through a defect in the calvarium. Encephalocele is the term used to describe herniation of the meninges and brain through the defect ; cranial meningocele describes the herniation of only meninges. Cephaloceles occur at a rate of 1 in 2000 live births (Hagen-Ansert, 2001).

2-2-4 Spina bifida:

Spina bifida encompasses a wide range of vertebral defects that result from failure of neural tube closure. Through this defect the meninges and neural elements may protrude. The defect may occur anywhere along the vertebral column but most commonly occurs along the lumbar and sacral regions. This

is the second most common open neural tube defect. When the defect involves only protrusion of the meninges, it is termed a meningocele. More commonly the meninges and neural elements protrude through the defect and are termed a meningomyelocele. If the defect is very large and severe, it is termed rachischisis. Sonographic features of spina bifida include, splating of the posterior ossification centers with a V or U configuration, Protusion of a sac like structure that may be an echoic (meningocele) or, contain neural elements(myelomeningocele), A cleft in the skin. The associated sonographic cranial findings include flattening of the frontal bones, giving the head a "lemon" shape; obliteration of the cisterna magna; inferior displacement of the cerebellar vermis, giving the cerebellum a rounded, "banana" shape ; ventriculomegaly. The " lemon sign" is not specific for spina bifida, and similar head shapes have been described with other CNS malformations, such as encephalocele, and non-CNS malformations, such as thanatophoric dysplasia. Other sonographic findings associated with spina bifida include talipes, cephaloceles, cleft lip and palate, hypotelorism, heart defects, and genitourinary anomalies (Hagen-Ansert, 2001).

2-2-5 Holoprosencephaly:

Holoprosencephaly encompasses a range of abnormalities resulting from abnormal cleavage of the prosencephalon (forebrain). The incidence is 0.6 in 1000 live births, although the incidence in embryos has been much higher (1 in 250). It is often associated with facial abnormalities, especially with the most severe forms. Other sonographic findings associated with holoprosencephaly include hydrocephaly, microcephaly, polyhydramnios, and intrauterine growth restriction (IUGR). In addition, renal cysts or dysplasia, omphalocele, cardiac defects, spina bifida, talipes, and gastrointestinal anomalies have been identified in the presence of holoprosencephaly (Hagen-Ansert, 2001).

2-2-6 Ventriculomegaly (hydrocephalus):

Ventriculomegaly refers to dilation of the ventricles within the brain. Hydrocephalus occurs when ventriculomegaly is coupled with enlargement of the fetal head. Fetal head enlargement when the biparietal and head circumference measurements exceed those for the established gestational age. The incidence of ventriculomegaly occurs in 0.5 to 1.8 per 1000 births. Enlargement of the ventricles occurs with obstruction of cerebrospinal fluid flow. Ventriculomegaly may also be associated with musculoskeletal anomalies such as thanatophoric dysplasia and achondroplasia. In addition to numerous intracranial abnormalities associated with ventriculomegaly, the fetus should be surveyed for defects involving the face, heart, kidneys abdominal wall, thorax, and limb (Hagen-Ansert 2001).

2-2-7 Microcephaly:

Microcephaly is an abnormally small head that falls 2 standard deviations below the mean. It occurs because the brain is reduced in size. Isolated microcephaly occurs in 1 per 1000 births but is more commonly caused by an associated anomaly. Sonographic features include a small head circumference, abnormal head circumference/abdomen circumference and head circumference to femur length ratios (Hagen-Ansert, 2001).

2-2-8 Omphalocele:

Because of the lack of space within the abdominal cavity and the large fetal liver and kidneys, the bowel is forced from the abdomen and into the extraembryonic coelom of the umbilical cord. These herniated loops of bowel normally return and rotate into position within the abdominal cavity by the 12th week of pregnancy. When bowel loops fail to return to the abdomen, a bowel-containing omphalocele occurs. This herniation is covered by a membrane that is composed of amnion and peritoneum. The omphaloceles are characterized as two types: those that contain the liver

within the sac and those that contain a variable amount of bowel, but no liver which affects the abdominal wall muscles, fascia, and skin. Liver omphaloceles may contain bowel and demonstrate a relatively large abdominal wall defect in comparison to the abdominal diameter (Hagen-Ansert, 2001).

2-2-9 Gastroschisis:

Gastroschisis is an opening in the layers of the abdominal wall with evisceration (herniation) of the bowel and, infrequently, the stomach, genitourinary organs. Gastroschisis defects are small (2 to 4 cm in size) and are located next to the normal cord insertion. In the majority of cases, the defect is positioned to the right of the umbilical cord. The insertion of the umbilical cord is normal in fetuses with gastroschisis. Small bowel is always found in the herniation. Other organs that may be involved in the herniation include the large bowel, the stomach, occasionally portions of the genitourinary system, and rarely the liver. The sonographer may be able to detect gastroschisis after 12 weeks of gestation. The edges of the bowel are irregular and free floating without a covering membrane, as is seen with omphalocele (Hagen-Ansert, 2001).

2-2-10 Amniotic band syndrome:

The amniotic band syndrome is the rupture of the amnion, which leads to entrapment or entanglement of the fetal parts by the "sticky" chorion. This may be cause amputation or defects in random sites. Early entrapment by the bands may lead to severe craniofacial defects and internal malformations. Late entrapment leads to amputations or limb restrictions (Hagen-Ansert, 2001).

2-2-11 Abnormalities of skeleton:

Skeletal dysplasia is the term used to describe abnormal growth and density of cartilage and bone. Dwarfism occurs secondary to a skeletal dysplasia and

refers to a disproportionately short stature. There are over 100 types of skeletal dysplasias, and not all of them are amenable to sonographic detection. The perinatal team may be able to isolate a skeletal dysplasia when abnormal skeletal structures are observed, such as bone shortening or hypomineralization. The sonographer should become familiar with the sonographic characteristics of the more common skeletal dysplasias that can be diagnosed in utero (Hagen-Ansert, 2001).

2-2-11-1 Sonographic evaluation of skeletal dysplasias:

The patient whose fetus is at risk for a skeletal dysplasia is commonly referred to a maternal-fetal center for genetic counseling and a targeted ultrasound. Although many skeletal dysplasias are inherited, sporadic occurrences and new mutations do occur, so it is important to screen for skeletal dysplasias as part of every obstetric ultrasound examination. The majority of prenatally diagnosed skeletal dysplasia occurs in association with polyhydramnios or other fetal anomalies or when there is a risk for recurrence. When a skeletal dysplasia is suspected, the protocol of the obstetric ultrasound examination should be adjusted to assess limb shortening. All long bones should be measured. A skeletal dysplasia is suspected when limb lengths fall more than 2 standard deviations below the mean; assess bone contour. Thickness, abnormal bowing or curvature, fractures, and a ribbon like appearance should be noted; estimate degree of ossification. Decreased attenuation of the bones with decreased shadowing suggests hypomineralization. Special attention should be focused toward this assessment of the cranium. Spine ribs, and long bones; evaluate the thoracic circumference and shape. A long, narrow chest or a bell-shaped chest may be indicative of specific dysplasias; survey for coexistent hand and foot anomalies such as talipes and polydactyly; evaluate the face and profile for facial clefts, frontal bossing, micrognathia, hypertelorism, and other facial anomalies that may be associated with skeletal dysplasias. Survey for other

associated anomalies such as hydrocephaly, heart defects, and nonimmune hydrops. The manifestation of skeletal dysplasias varies based on the specific dysplasia. Long bones are affected in different patterns (Figure 2.17) according to the dysplasia. Rhizoma is shortening of the proximal bone segment(humerus and femur). Mesomelia refers to shortening of the middle segments (radius/ulna and tibia/fibula). Micromelia describes the shortening of the entire extremity (Hagen-Ansert, 2001).

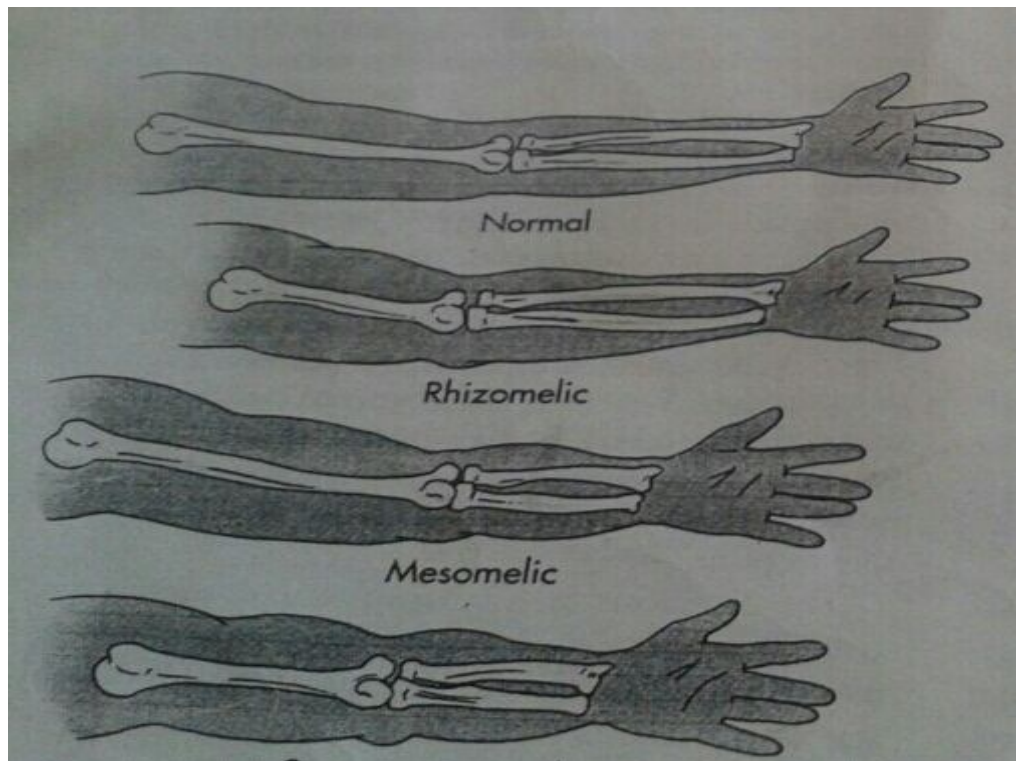


Figure (2.17) diagram illustrates Varieties of short-limb dysplasia according to the affected bones. Rhizomelic dyaplasia is characterized by shortening of the proximal long bones (humerus and femur).Mesomelic dysplasias is described as shortening of the distal extremities (radius/ulna and tibia/fibula). Severe micromelia produces shortening of both proximal and distal extremities(Hagen-Ansert, 2001).

Sonographic examination of the long bones should include an assessment to define whether there is segmental shortening or micromelia, because this is will aid in the diagnosis (Hagen-Ansert,2001).

2-2-11-2 Thanatophoric dysplasia:

Thanatophoric dysplasia is the most common lethal skeletal dysplasia and occurs in 1 in 10,000 birth. The term thanatophoric comes from the Greek word thanatophoros, which means death bearing. The two main subdivisions of thanatophoric dysplasia are types I and II. Type I is characterized by short, curved femurs and flat vertebral bodies, and a cloverleaf skull. The sonographic features include severe micromelia (Figure 2.18, A and B), especially of the proximal bones (rhizomelia) ; cloverleaf deformity, Kleeblattschadel skull, occurs in 14% of thanatophoric fetuses as a result of premature craniosynostosis; narrow thorax with shortened ribs (Figure 2.18, C and D); protuberant abdomen; frontal bossing (bulging forehead); and hypertelorism (widely spaced eyes); flat vertebral bodies(platyspondyly) (Hagen-ansert, 2001).



Figure (2.18) ultrasound image illustrates lethal skeletal dysplasia consist with thanatophoric dysplasia at gestational age of 18 weeks,1 day. A and B, The right arm demonstrates micromelia. The lower extremities were also short, with the femurs measuring gestational age 14 weeks. C, The thorax was very narrow. D,, The ribs were short. The abdomen was protuberant (E) and compared with the narrow thorax(Hagen-Ansert, 2001).

Other sonographic findings that may be associated with thanatophoric dysplasia include severe polyhydramnios, hydrocephalus, and nonimmune hydrops (Hagen-Ansert,2001).

2-2-11-3 Achondroplasia:

Achondroplasia is the most common nonlethal skeletal dysplasia. It result from decreased endochondral bone formation which produces short, squat bones. The sonographic features of achondroplasia may not be evident until after 22 weeks of gestation, when biometry becomes abnormal. Ultrasound findings include rhizomelia, macrocephaly, trident hands (short proximal and

middle phalanges), nasal bridge, frontal bossing, and mild ventriculomegaly may be identified (Hagen-Ansert, 2001).

2-2-11-4 Achondrogenesis:

It is caused by cartilage abnormalities that result in abnormal bone formation and hypomineralization. The sonographic features include severe micromelia, decreased or absent ossification of the spine, macrocephaly, short trunk, short thorax and short ribs, micrognathia, hydrops possibly identified (Hagen-Ansert, 2001)

2-2-11-5 Osteogenesis imperfecta:

Osteogenesis imperfecta is a disorder of collagen production leading to brittle bones; manifestations in the teeth, skin, ligaments; and blue sclera. There are four classifications, types I to IV. Types I and IV are the mildest forms, and it would be unlikely that a diagnosis would be made in utero. The sonographic features of osteogenesis imperfect type II include generalized hypomineralization of the bones, especially the calvarium; multiple fractures of the long bones, ribs, and spine; narrow thorax, and micromelia (Figure 2.19) (Hagen-Ansert, 2001)

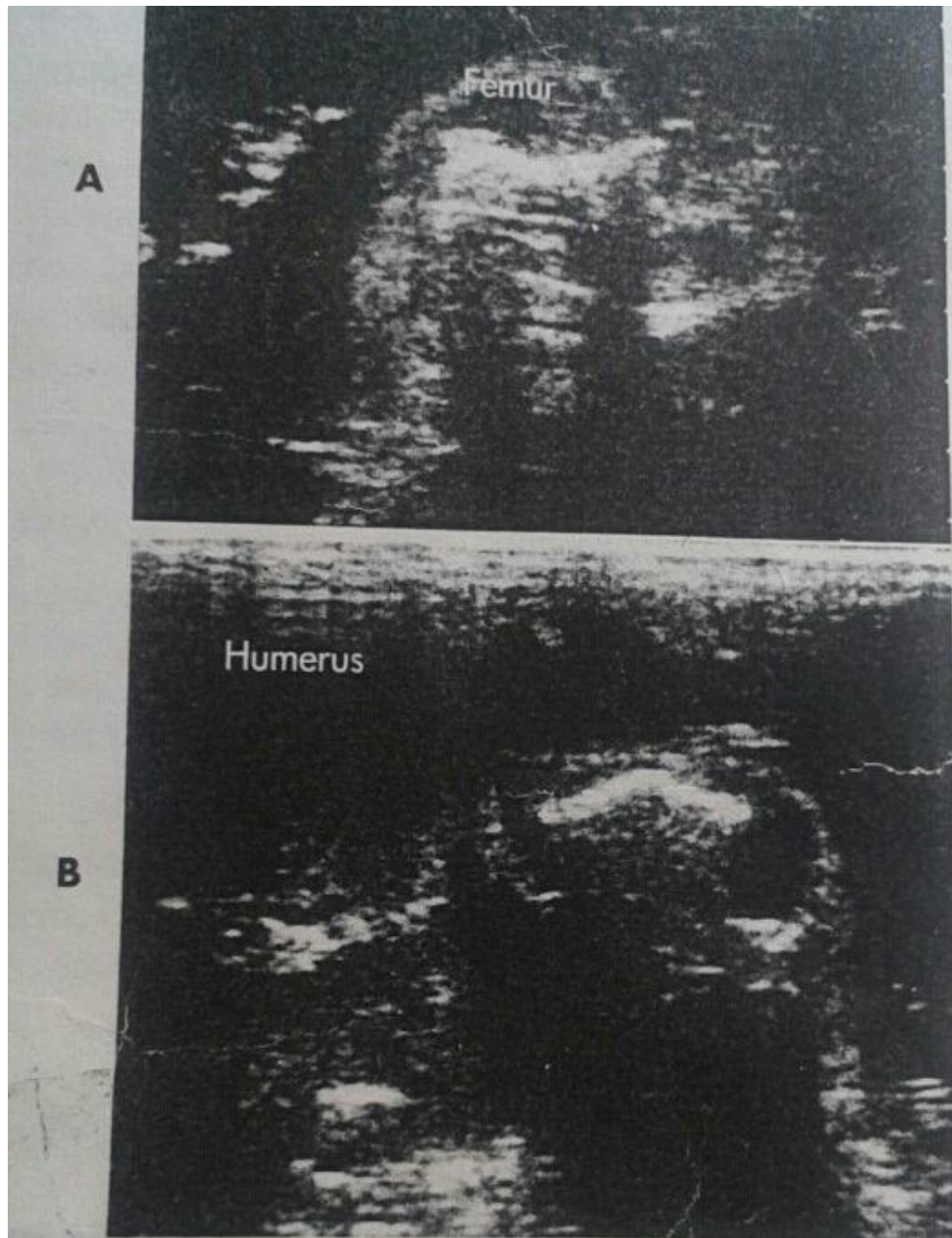


Figure (2.19) ultrasound image illustrates A, marked micromelia in a 30-week fetus with osteogenesis imperfecta (type II). The femur measured 29mm (normal for 30 weeks is 57mm). B, In the same fetus a humeral fracture is shown. Humeral length measured 27mm (normal for 30 weeks is 51mm) (Hagen-Ansert, 2001).

The multiple fractures that have occurred during the course of pregnancy may leave the bones bowed, thickened, and sharply angulated.

Polyhydramnios may also be evident. The sonographic features of osteogenesis imperfecta type III are similar to those of type II, though it is less severe (Hagen-Ansert,2001).

2-2-11-6 Congenital hypophosphatasia:

Congenital hypophosphatasia is a condition that presents with diffuse hypomineralization of the bone caused by an alkaline phosphatase deficiency. The sonographic features include diffuse hypomineralization of the bones; moderate to severe micromelia; extremities that may be bowed, fractured, or absent ; poorly ossified cranium with well-visualized brain structures, and small thoracic cavity (Hagen-Ansert,2001).

2-2-11-7 Diastrophic dysplasia:

Diastrophic dysplasia is a very rare disorder characterized by micromelia, talipes, cleft palate, micrognathia, scoliosis, short stature, earlobe deformities, and hand abnormalities. The sonographic features include micromelia, hand abducted thumb (thicker thumb), talipes (clubfoot), micrognathia (small chin), and cleft palate (Hagen-Ansert,2001).

2-2-11-8 Camptomelic dysplasia:

Camptomelic(bent bone) dysplasia is a group of lethal skeletal dysplasias that are characterized by bowing of the long bones. The sonographic features include bowing of the long bones with lower extremities affected most severely(Figure 2.20), small thorax, hypoplastic fibulas, hypertelorism, cleft palate, micrognathia, talipes, ventriculomegaly, and hydronephrosis (Hagen-Ansert,2001).

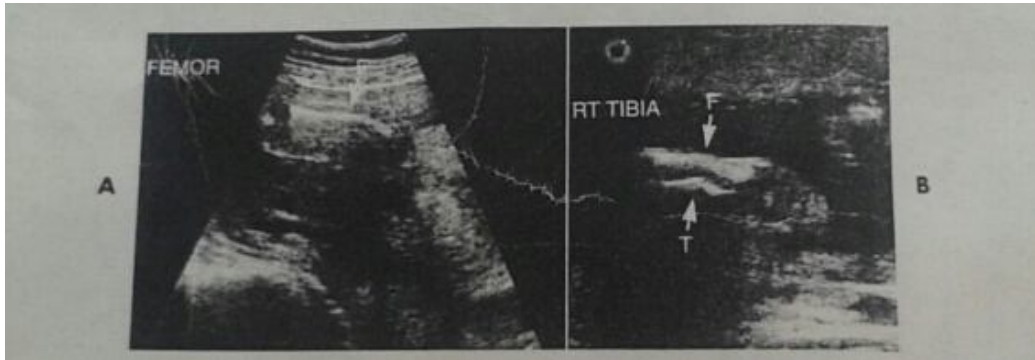


Figure (2.20) ultrasound image illustrates A, Camptomelic dysplasia in 20-week fetus with femoral bowing (F) found bilaterally. The femoral lengths were normal. B, in the same fetus, the tibias (T) were short and hypoplastic. The fibulas (F) were hypoplastic and bowed (Hagen-Ansert, 2001).

2-2-11-9 Roberts' syndrome:

Roberts' syndrome is rare condition characterized by phocomelia and facial anomalies. The sonographic features include phocomelia with the upper extremities more severely affected, bilateral cleft lip and palate, hypertelorism, microcephaly, and cardiovascular, renal, and gastrointestinal anomalies may be identified (Hagen-Ansert,2001).

2-2-11-10 Short-rib polydactyly syndrome:

Short-rib polydactyly syndrome is lethal skeletal dysplasia characterized by short ribs and polydactyly. There are four types. Common sonographic features include narrow thorax with short ribs, polydactyly, micromelia, and midline facial cleft. Other sonographic findings associated with short-rib dysplasias include anomalies of the central nervous system, cardiovascular system, and genitourinary tract. Polyhydramnios may also be identified. Type I and III are usually not associated with cleft lip and palate, and polydactyly may not always be present in type IV (Hagen-Ansert,2001).

2-2-11-11 Jeune syndrome:

JEUNE syndrome, also known as asphyxiating thoracic dysplasia, is skeletal dysplasia characterized by a very narrow thorax. The sonographic features

include small thorax, rhizomelia, renal dysplasia, and polydactyly (Hagen-Ansert,2001).

2-2-11-12 ELLIS-VAN CREVELD syndrome:

ELLIS-VAN CREVELD syndrome is also known as chondroectodermal dysplasia. The sonographic features include limb shortening, polydactyly, and heart defects (50%) (Hagen-Ansert,2001).

2-2-11-13 Caudal regression syndrome/Sirenomelia:

Caudal regression syndrome includes a range of malformations from sacral agenesis to sirenomelia, in which there is fusion of the lower extremities (Hagen-Ansert,2001).

2-2-11-13-1 Sonographic features of caudal regression include the following:

Sacral agenesis, talipes, abnormal lumbar vertebrae, pelvic abnormalities, and contractures or decreased movement of the lower extremities may also be seen (Hagen-Ansert,2001).

2-2-11-13-2 Sonographic features of sirenomelia include the following:

Variable fusion of the lower extremities, bilateral renal agenesis, oligohydramnios, and single umbilical artery (Hagen-Ansert,2001).

2-2-12 VACTERL association:

The vacteral association is a group of anomalies that may occur together, which are Vertebral defects, Anal atresia, Cardiac anomalies, TracheoEsophageal fistula, Renal anomalies, and Limb dysplasia.

A single umbilical artery has also been noted in association with VACTERL (Hagen-Ansert,2001).

2-2-13 Arthrogryposis multiplex congenital:

Is a condition marked by severe contractures of extremities because of abnormal innervation and disorders of the muscles and connective tissues. The sonographic findings include rigid extremities, flexed arms,

hyperextension of the knees, clinched hands, and talipes (Hagen-Ansert,2001).

2-2-14 Lethal multiple pterygium syndrome:

Is characterized by webbing across the joints and multiple contractures. The sonographic findings include limb contractures, webbing across joints, and cystic hygroma. Micrognathia, hydrops, and polyhydramnios are also associated with this syndrome(Hagen-Ansert,2001).

2-2-15 Pena-Shokeir syndrome:

Is characterized by abnormal joints contractures, facial abnormalities, polyhydramnios, intrauterine growth restriction, and pulmonary hypoplasia. The sonographic findings (fig. 2-21) include limb abnormalities such as contractures, clinched hands, and talipes; facial abnormalities, including micrognathia, and cleft palate. Polyhydramnios and hydrops may also be identified (Hagen-Ansert,2001).



Figure (2.21)An ultrasound image at 19 weeks of gestation revealed rigid legs with the knees hyperextended (A). The arms were contracted and crossed over the chest with hands clenched polyhydramnios and micrognathia were also noted (Hagen-Ansert, 2001).

2-2-16 Miscellaneous limb abnormalities:

The prevalence of limb abnormalities is approximately six in 10,000 live births, the incidence is higher in the upper limbs compared with the lower limbs (3.4 of 10,000 and 1.1 of 10,000,respectively) (Johnson etal, 2005).

Limb abnormalities are more commonly unilateral than bilateral and more frequently in the right limb compared with the left (Granellini et al,2005).

Patient body habitus, quality of the ultrasound machine, and operator skill have the main role in the detection and diagnosis of limb abnormalities using prenatal ultrasonography (Emanuel et al,1995).

Limb abnormalities can be isolated or associated with other malformation and detected as part of a known syndrome (chromosomal or single gene), in the latter case they are diagnosed more accurately than in former one(Emanuel et al,1995 & Espinasse et al,1996).

2-2-16-1 Chromosomal disorders associated with limb abnormalities:

Trisomy 21 associated with Short broad hands, clinodactyly and short fifth fingers, “sandal gap,” slightly short femur and humerus; Trisomy 13 associated with Postaxial polydactyly, clenched hands, overlapping fingers, prominent Heels; Trisomy 18 associated with Radial ray defects, hypoplastic thumbs, clenched hands, overlapping fingers, “rocker bottom feet,” clubhand, clubfeet, ectrodactyly, prominent heels, dislocated hips; del(4) associated with Clubfeet; del(5) associated with Clinodactyly of the fifth fingers, clubfeet, syndactyly of the second and third fingers and toes, oligosyndactyly, hyperextensible joints; Trisomy 8 associated with Camptodactyly of second to fifth fingers, joint contractures; Triploidy Syndactyly of the third to fourth fingers, “sandal gap”, clubfeet and Del(3) associated with Postaxial polydactyly (Lazebnik, 2008).

2-2-16-2 Nomenclature used in defining the type of limb defect:

Acheiria, absence of hand(s); acromelia, Shortening of a distal segment in hands/feet; adactyly, absence of fingers/toes; amelia, absence of a limb(s)
Apodia, absence of foot/feet; brachydactyly, abnormally short fingers
Camptomelia, bent limb; clinodactyly, in turning of a finger; hemimelia, absence of a longitudinal segment of a limb; mesomelia, shortening of a middle segment in hands/feet; micromelia, Shortening of all long bones; oligodactyly, partial loss of fingers; phocomelia, hypoplasia of the limbs (hands attached to shoulders, feet to hips); polydactyly, supernumerary digits; rhizomelia, shortening of a proximal segment in upper/lower limbs (humeri/femurs); syndactyly, fused digits; terminal transverse defects, absence of distal structures of the limb with normal proximal structure; proximal intercalary defects, absence or severe hypoplasia of proximal intercalary parts of the limb where the distal parts of the limb (normal or malformed), are present; longitudinal absence or severe hypoplasia of a lateral part of the limb, absence of a lateral component of a limb; split hand/foot, (ectrodactyly) absence of central digits with or without absence of central metacarpal/metatarsal bones. Usually associated with syndactyly of other digits (Lazebnik, 2008).

2-2-16-2-1 Clinodactyly:

Clinodactyly is a fixed deviation of the fingers or toes. Clinodactyly of the toes is difficult to detect on fetal ultrasound scan; thus, the review concentrates on clinodactyly of the fingers. This abnormality affects each of the fingers but is most commonly seen as fifth finger clinodactyly (Lazebnik, 2008).

2-2-16-2-2 Camptodactyly:

Camptodactyly is a flexion contracture of one of the interphalangeal joints. Prenatally, only affected fingers can be diagnosed (Lazebnik, 2008).

2-2-16-2-3 Phocomelia:

In phocomelia, the hands or feet are present, but the arms/forearms and thighs/calves are missing or foreshortened. The hands/feet may be normal or abnormal (Lazebnik, 2008).



Figure (2.22) Prenatal ultrasound scan of a fetus at 14 weeks with tetramelia and hydrops. Thin arrow, scapula; thick arrows, absent upper limbs; arrow-head, left pleural effusion (Lazebnik, 2008).

2-2-16-2-4 Clubhand:

This condition is divided into radial and ulnar form. Radial and ulnar clubhand are frequently associated with radial ray and ulnar ray abnormalities, respectively (Taybi&Lachman,1996 &Romero et al,1990).

Radial clubhand is more commonly detected prenatally and very often is associated with other abnormality, many of them inherited. Ulnar clubhand is secondary to ulnar ray deficiency. This is a rare anomaly and is usually isolated, although it can be association with TAU syndrome (thrombocytopenia and absent ulna with mental retardation and facial dysmorphism) (Stoll et al,1992).

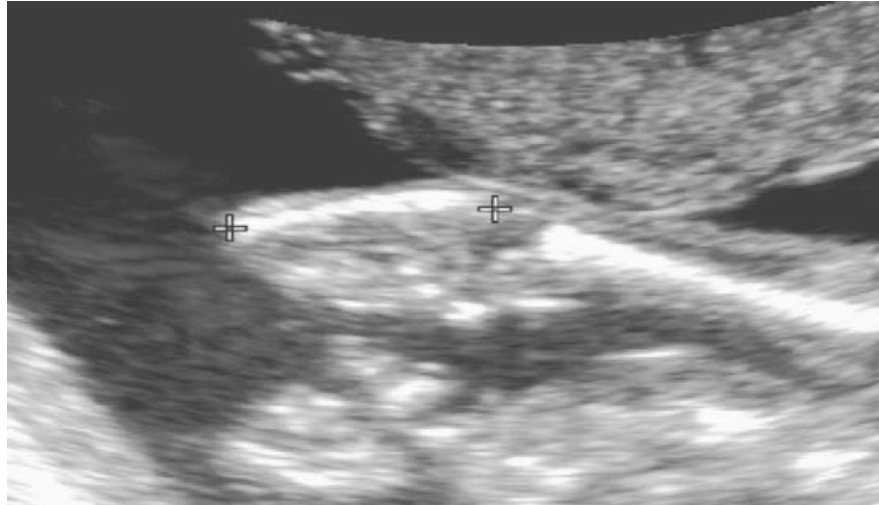


Figure (2.23) ultrasound image shows Clubhand. Humerus is normal. Forearm has single short bone. Hand and wrist are flexed acutely and lie along anterior aspect of forearm. Fetus has trisomy 18 (Lazebnik, 2008).

2-2-16-2-5 Clenched Hand:

Clenched hand (the second and fifth fingers overlap the third and fourth with an adducted thumb) seen on fetal ultrasound scan must be evaluated carefully to determine that it is a persistent and not a temporary finding (Lazebnik, 2008).



Figure (2.24)Ultrasound scan shows finger clenching in fetus (Lazebnik, 2008).

2-2-16-2-6 Thumb Anomalies:

The prenatal diagnosis of thumb abnormalities includes thumb hypoplasia, triphalangeal thumb, broad thumb, and hitchhiker thumb. Thumb abnormalities may be isolated but in most cases are associated with other body organ or limb abnormalities. The extremely rare hitchhiker thumb deformation corresponds to the abnormally abducted position of a more proximally inserted thumb (Lazebnik, 2008).

2-2-16-2-7 Polydactyly:

Polydactyly consists in the presence of extra digit/s in the upper or lower extremities (Figure 2-25). The extra digits may vary in their developmental maturity. The extradigit can appear on the radial side (preaxial) or on the ulnar side (postaxial) polydactyly (Lazebnik, 2008).

Meso-axial polydactyly is less frequent than pre-/postaxial polydactyly. Postaxial polydactyly is more frequent than preaxial polydactyly, particularly among Africans. The incidence of polydactyly is one in 700 pregnancies (Teot & Deschamps, 1990).

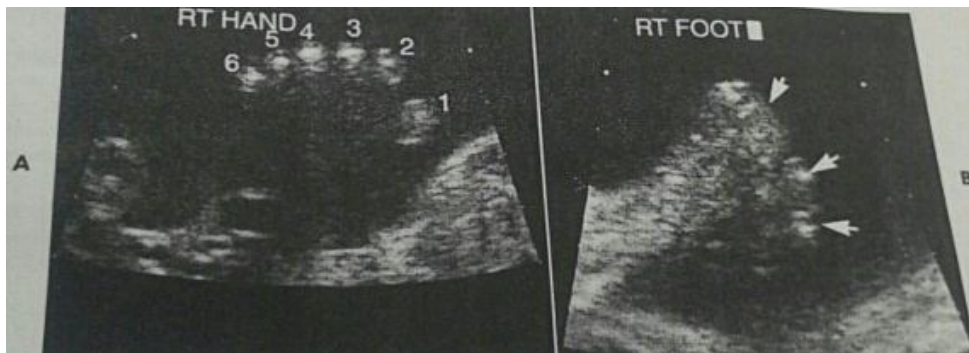


Figure (2-25) ultrasound image shows A, polydactyly (six fingers) in a 26-week of fetus. B, In the same fetus, duplication of the great toe (arrows) is shown (Hagen-Ansert, 2001)

2-2-16-2-8 Terminal Transverse Limb Defects:

Generally, terminal transverse defects are more common in the upper limbs than the lower limbs; they may be isolated or part of syndromes and are likely to be associated with other abnormalities. The condition is thought to

result from a vascular injury and has been found in association with coagulation defects. In many cases the condition is the result of constriction band sequence/amniotic band sequence, caused by early rupture of the amnion and formation of fibrous bands that can trap, constrict, and disrupt fetal parts. The presentation can vary from a simple circumferential groove to ring constriction, amputation of part of a finger resulting in whole-limb amputation, or severe malformations including syndactyly, pterygium, and lethal craniofacial or thoraco-abdominal destructive possesses. Disruptions caused by amniotic bands are characterized asymmetrical and are a menable to ultrasound detection (lazebnik, 2008).

2-2-16-2-9 Ectrodactyly (Split hand/foot):

Split hand/foot deformity, also known as lobate claw hand/foot, results from a bsence of the central digits/toes with a deep V- or U-shaped central cleft. The main pathogenic mechanism is most probably a failure of the median apical ectodermal ridge in the developing limb bud.(Duijfet al 2003).

It may be isolated or associated with other abnormalities such as in EEC syndrome(ectrodactyly,ectodermal dysplasia, cleft lip/palate) and syndactyly, absence, or hypoplasia of the residual phalanges; metacarpals/metatarsal can also be seen (Elliott et al,2005).



Figure (2.26) ultrasound image shows ectrodactyly. Thumb is visible on one side of the V defect. Malformed fingers on the other side (Lazebnik, 2008).

2-2-16-2-10 Syndactyly:

In Syndactyly two or more digits are fused together. It is the most common congenital malformation of the limbs, with an incidence of 1 in 2000 to 3000 live births (Lamb et al, 1982 & Light, 1996).

The condition is the result of failure of separation of the fingers or toes into individual appendages, which usually occurs between the sixth and seventh week postconception. It is defined as simple when it involves soft tissue only or complex when it involves the bone or nail of the adjacent fingers or toes that are joined side by side. It can be complete when the fusion extends to the tip of the finger or toe or incomplete when the soft-tissue union does not extend to the finger tips. Complex syndactyly refers to fingers joined by bone or cartilaginous union, usually in a side-to-side fashion at the distal phalanges. The most severe form of syndactyly is classified as complicated syndactyly which refers to fingers joined by bony fusion other than side-to-side and can include bony abnormalities such as extra, missing, or duplicated phalanges and abnormally shaped bones such as delta phalanges. The complex type of syndactyly may be associated with other finger or toe abnormalities including polydactyly, oligodactyly, or duplicated (Iazebnik, 2008).

2-2-16-2-11 Clubfoot (talipes):

is one of the most common congenital birth defects and has been diagnosed as early as 13 weeks' gestation by transvaginal sonography (Bar-Harval et al, 1997 & Bronshtein, 1989) and at 16 weeks by transabdominal ultrasound scan (Benacerraf, 1986).

Clubfoot may be identified sonographically when there is persistent abnormal inversion of the foot perpendicular to the lower leg (Figure 2-27) (Hagen-Ansert, 2001).



Figure 2.27 clubfoot identified during a basic scan in a 19 week fetus.
Note the medial inversion of the foot (F) in relation to lower leg (L)
(Hagen-Ansert,2001).

2-3 Ultrasound physics and equipment:

2-3-1 Ultrasound physics:

Ultrasound waves move in a longitudinal forward motion and require a medium (solid, liquid, or gas) in order to propagate. As they travel through the medium, they cause disturbances that consist of alternate compressions and rarefactions. One compression and one rarefaction is equal to one wave length (Fig. 2.28). When the frequency increases the wave length decreases. Higher frequencies with shorter wave lengths are used in clinical practice to produce the greatest detail and resolution. However, a limiting factor is the loss of penetration (increased attenuation). Therefore, we use the highest frequency possible that will sufficiently penetrate the body structures (Krebs et al, 1993).

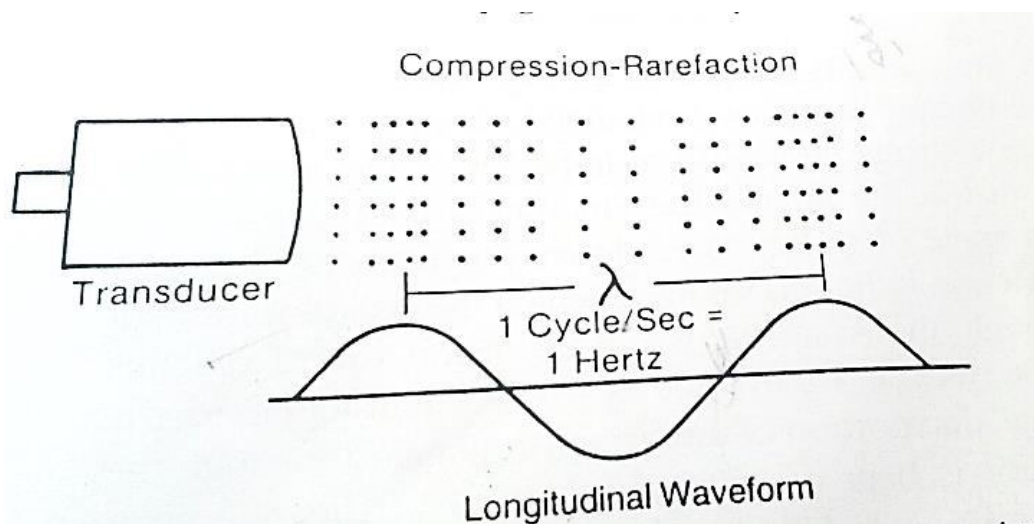


Figure (2.28) diagram shows Longitudinal waveform with compressions and rarefactions (Krebs et al, 1993).

The medium through which the sound wave is traveling governs many of the events that occur. The compressibility of the medium determines how the sound is propagated. Harder substances impede propagation of the wave and have a high acoustic impedance, compared to softer materials that have low acoustic impedance. The acoustic impedance is the material property directly involved with echo production. Note that if there is no impedance there is no

echo return. The greater the mismatch of tissue densities (impedance) the greater the amplitude of the return echo. To eliminate large reflections at air-solid or air-liquid interfaces, a coupling agent is used to avoid any air space between the transducer and the body. Attenuation is defined as the amount of energy lost from the sound beam per unit depth. A sound can be attenuated by the imparting of heat to the tissue through which the beam travels. This loss of energy causes the beam to decrease in intensity. The beam also uses energy as it is refracted and is scattered as it travels through the medium. As the sound beam moves through tissue, a portion of the energy is reflected whenever there is an interface with a change in acoustical impedance. The greater the mismatch, the greater the amount of energy reflected. The angle of reflection is always equal to the angle of incidence. If the surface upon which the incident ray falls is rough, the scattering is diffuse. If the sound reaches an interface and the angle is not perpendicular to the surface, that portion of the beam propagated through the interface is bent or refracted. Not all of the energy is refracted. Some of the energy will be scattered in several directions. The best echo return is achieved when the transducer axis is perpendicular to the interface so that the maximum reflected energy can pass through the transducer (Figure 2.29) (Krebs et al, 1993)

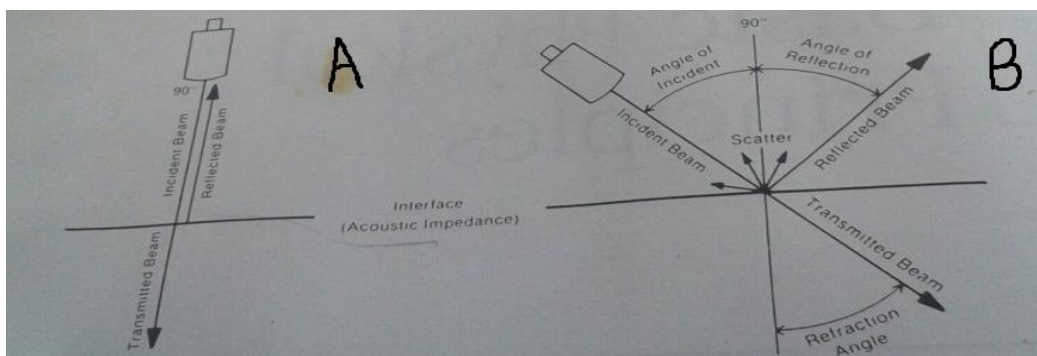


Figure (2.29) Schematic of propagation, reflection and refraction. (A) Reflections without refraction. (B) Reflection with refraction (Krebs et al, 1993).

Diagnostic ultrasound, which operates in a frequency range of 1 to 20 megahertz (MHz), is generated by transducers that transform electrical energy into ultrasonic energy. The transducers are most commonly made of piezoelectric crystals, which use piezoelectric effect to convert a voltage to a mechanical strain. The application of an oscillatory voltage across the crystal causes it to vibrate, which in turn creates a series of compressions and rarefactions in the adjacent media leading to generation of the ultrasound beam (Krebs et al, 1993).

2-3-1-1 Basic principle of ultrasound:

Ultrasound is the name given to high-frequency sound waves, over 20000 cycles per second (20 kHz). These waves, inaudible to humans, can be transmitted in beams and are used to scan the tissues of the body. Different tissues alter the waves in different ways: some reflect directly while others scatter the waves before they return to the transducer as echoes. The waves pass through the tissues at different speeds (for example, 1540 metres per second through soft tissues). The reflected ultrasound pulses detected by the transducer need to be amplified in the scanner. The echoes that come from deep within the body are more attenuated than those from the more superficial parts. And therefore require more amplification. Ultrasound scanners have controls to change amplification of the echoes from different depths. When working with any scanner it is necessary to achieve a balanced image. One that contains echoes of approximately equal strengths from all depths of tissue. When the echoes return to the transducer, it is possible to reconstruct a two-dimensional map of all the tissues that have been in the beams. The information is stored in a computer and displayed on a video (television) monitor. Strong echoes are said to be of “high intensity” and appear as brighter dots on the screen, that is refers only to ultrasound used for medical diagnosis. Tissues vary greatly in their effect on ultrasound. For example, the skeleton and gas in the bowel or chest behave very

differently from soft tissue. When ultrasound waves meet bone or gas in the body, they are significantly reflected and refracted. Thus, it is usually impossible to use ultrasound effectively when there is a lot of gas in the bowel: when examining the pelvis the urinary bladder should be as full as possible to lift the intestine out of the way. Because of the effect of air, the normal lungs cannot be examined at all by ultrasound, but pleural fluid or amass in contact with the chest wall can be imaged. The skeleton reflects ultrasound so strongly that the architecture within a bone or heavily calcified tissue cannot be seen and there is an acoustic shadow behind it(Breyer et al, 1995).

2-3-2The ultrasound equipment, component and their uses:

Real-time equipment currently available varies greatly in size, shape and complexity, but will contain five basic components: the probe, in which the transducer is housed, the control panel, the freeze frame, measuring facilities, and a means of storing images.Current equipment provides 2D or threedimensional(3D) information(Chudleigh and Thilaganathan, 2004).

2-3-2-1 The probe:

This refers to the piece of equipment in which the transducer (or transducers) is mounted. The transducer is a piezoelectric crystal that, when activated electronically, produces pulses of sound at very high frequencies – this is known as ultrasound. The crystal can also work in reverse in that it can convert the echoes returning from the body into electrical signals from which the ultrasound images are made up. In practise, however, the terms ‘probe’and ‘transducer’ are used interchangeably. The probe can either be a conventional type used externally or an intracavity type, such as that used transvaginally (Chudleigh and Thilaganathan, 2004).

The transabdominal transducer: is linear array, sector, and convex. In obstetric ultrasound the transducer should be linear or convex (Breyer et al, 1995).

These terms refer to the way in which the crystal or crystals are arranged and manipulated to produce an image. Transducers transmit ultrasound over a range of frequencies but all will have a central frequency (or band of frequencies) that defines the frequency of that probe. Ultrasound frequencies are described in megahertz (MHz). Transabdominal probes used in obstetrics typically have frequencies of 3.5 MHz or 5 MHz, whereas transvaginal probes can utilize higher frequencies of 7.0 MHz or 8.0 MHz. The important principle to remember is that frequency is related to image resolution but inversely related to penetration of the sound beam into the tissue being insonated. Thus the higher the frequency of the probe, the better the resolution of the image but the shallower the depth of tissue that can be examined. Transvaginal imaging can utilize higher probe frequencies because the area of interest, e.g. the ovary, the cervical canal and internal os, non-pregnant or early pregnant uterus, is much closer to the transducer – and therefore the sound source – than with a transabdominal probe (Chudleigh and Thilaganathan, 2004).

2-3-2-2 The control panel:

Ultrasound, can be regulated by a volume control that, is known as a gain control. The amount of sound produced by the transducer and transmitted into the patient by the machine is determined by the overall gain control. The information obtained from the echoes returning to the transducer from the patient and received by the transducer is manipulated by the receiver gain and the time gain compensation controls. As acoustic exposure is determined by the amount of sound transmitted into the patient the overall gain control should be kept as low as possible. The amplification of the returning echoes is known as time gain compensation (TGC). In most machines, TGC is

manipulated by a series of sliders that control slices (of, typically, 2 cm in depth) of the image. The receiver gain control or TGC settings are crucial in the quality of the image displayed. Too little gain produces a very dark image whereas too much gain produces too bright an image. Inappropriate settings of the TGC will produce dark and/or light bands within the image. The correct gain settings produce the image shown in (Figure 2.30) (Chudleigh and Thilaganathan, 2004).



Figure(2.30) ultrasound image shows Correct gain control settings. Notice how much more detail is seen from the structures within the fetal abdomen (Chudleigh and Thilaganathan, 2004).

Structures can be identified more easily and the margin of error in measurement is less when a large image size is used. It is good practice always to scan and record images using as large an image as is comfortably possible (Chudleigh and Thilaganathan, 2004).

2-3-2-3 Freeze-frame control:

This is essential for taking measurements and for storing images. The position of the control varies. It can be positioned on the control panel or, most conveniently, as a foot switch. An experienced operator always has a finger within instant striking distance of the control panel freeze-frame

control, or a foot resting on the freeze-frame foot switch (Chudleigh and Thilaganathan, 2004).

2-3-2-4 Measuring facilities – onscreen measurement:

All machines provide facilities for linear, circumference and area measurements. Measurements can be displayed alone or together with an interpretation of, for example, gestational age or fetal weight when an obstetric calculation preset program is selected. The gestational age given will vary depending upon the charts programmed into the machine. We recommend that sonographers interpret the measurements from each examination themselves, rather than relying on the information produced by the machine. The majority of caliper systems are of the roller ball or joy stick types. As with all technique on screen measuring requires expertise and it is therefore good practice to take several (we suggest three) measurements of any parameter to ensure accuracy. The monitor Ideally, there should be two monitors: a monitor for the operator and a second monitor for the parents or patient. Separate monitors allow both parties to view the examination comfortably and reduces considerably the risk to the operator of ergonomic related repetitive strain injury. If only one monitor is available, this should be positioned directly in front of the operator and not angled towards the woman, which would necessitate the operator straining his or her neck to view the screen (Chudleigh and Thilaganathan, 2004).

2-3-2-5 Storing the images – recording systems:

Digital storage and/or video tape recording are the preferred methods for making a permanent record of interesting or abnormal images (Chudleigh and Thilaganathan, 2004).

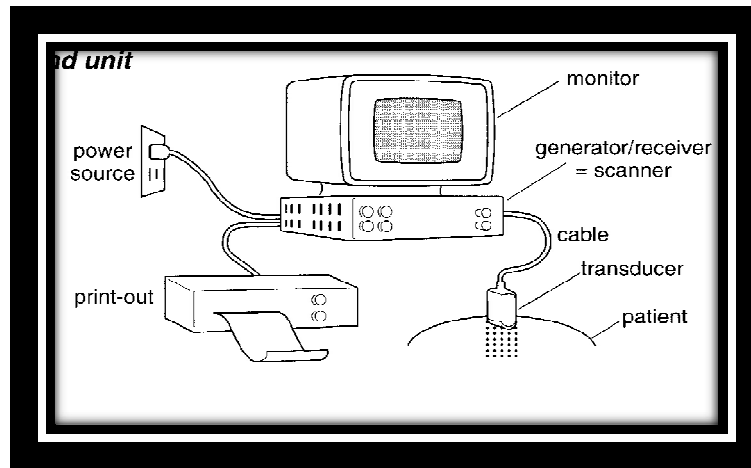


Figure (2-31) diagram shows complete ultrasound unit(Breyer et al,1993)

2-4 Sonographic technique:

The real time obstetric ultrasound examination is usually performed with the pregnant patient in the supine position. Sonogram gel is applied to the transabdominal or transvaginal transducer. The gel simulates a liquid interface that permits optimum travel of the sound waves (Kurjak and Chervenak, 2003)

2-4-1 Transvaginal method:

This is the preferred method for imaging the non-pregnant or early pregnant uterus. The preparations required for a transvaginal examination are an empty bladder, apply a small amount of gel to the transducer tip, and cover the tip and shaft of the probe with a (non-spermicidal) condom, and Apply a small amount of gel, or KY jelly, to the covered probe to allow easier insertion into the Vagina. Check that the left-right and top-bottom invert controls are activated such that the sector image on the monitor is orientated to your preference before you begin. Ensure that the selected image size is appropriate and that the zoom control is not activated. Hold the prepared probe with the mark or guide positioned to produce a longitudinal view of the pelvis. This usually means having the mark upper most. Insert the probe gently into the vagina. The uterus will usually be visualized by panning the

tip of the probe slightly towards the woman's right shoulder (to compensate for dextrorotation) By gently panning the probe to left and right, the optimal longitudinal view of the uterus should be obtained. The section of the uterus that is obtained by rotating the probe through 90° from the sagittal plane might be a coronal section of the uterus (Chudleigh and Thilaganathan, 2004).

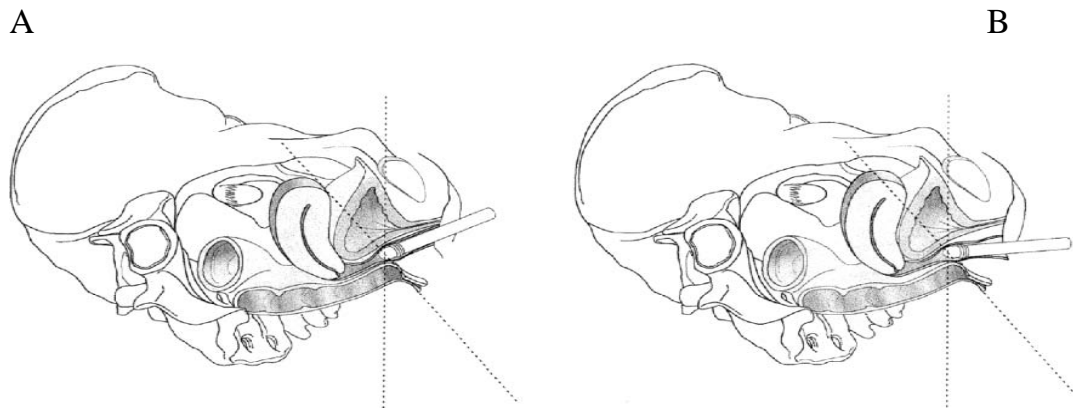


Figure (2.32) diagram shows Scanning planes that can be obtained with the transvaginal probe. A. sagittal or vertical plane; B. coronal or horizontal plane (Chudleigh and Thilaganathan, 2004).

2-4-2 Abdominal method:

To perform a pelvic ultrasound examination using the abdominal route, the woman must have a full bladder. This has three effects: first, it pushes the uterus out of the pelvis, thus removing it from the acoustic shadow caused by the symphysis pubis; second, it provides an acoustic window through which the pelvic organs can be visualized; third, it displaces the bowel superiorly, so preventing gas from the bowel scattering the ultrasound beam. Before you begin, check that you are holding the probe and/or that the left-right control is activated. Place the probe on the abdomen in the midline, immediately superior to the symphysis pubis to obtain longitudinal section of the pelvis. Cross-sectional views of the uterus are obtained by rotating the

probe through 90°. Sliding the probe up and down the abdomen will produce transverse sections of the uterus from fundus to cervix (Chudleigh and Thilaganathan, 2004).

In determining fetal position and in surveying the uterine contents the transducer is systematically toward the uterine fundus, maintaining a midline path. By moving the probe from side to side, fetal position, cardiac activity, the number of fetuses, the presence of uterine and placental masses, and any obvious fetal anomalies may be recognized and the amniotic fluid assessed (Hagen-ansert, 2001).

Knowing the relationship of the longitudinal axis of the fetus to the maternal abdomen establishes fetal lie, is necessary to confirm normal fetal situs and is an important preliminary to obtaining accurate measurements of the fetal head and abdomen (Chudleigh and Thilaganathan, 2004).

2-5 Obstetric measurements and gestational age :

The most accurate way to calculate the length of pregnancy is by knowing the date of conception. Delivery would then be expected to occur 38 weeks(266 days) later. However, as most women are unaware of the date of conception, the first day of the last menstrual period (LMP) is used to calculate the expected date of delivery (EDD). This is done by applying Naegele's formula to the LMP as follows: add 7 to the days, subtract 3 from the months, add 1 to the years. For example, if the LMP is 13.4.04 then the EDD is (13 +7). (4 -3). (04 +1), that is 20.1.05. This means that pregnancy is 40 weeks (280 days) long and assumes that conception occurs 2 weeks after the LMP. The LMP is unreliable (and therefore formula cannot be used) if the date of the LMP is not accurately known, menstrual cycle is not 28 days long, menstrual cycle is irregular, woman has only stopped taking the combined oral contraceptive pill ('the pill') within the last 3 months, woman has bled in early pregnancy, woman is breast feeding or has been pregnant in the preceding 3-6 months (Chudleigh and Thilaganathan, 2004).

2-5-1 Crown rump length measurement measurement (C R L):

The crown-rumplength is the most reliable parameter for estimating gestational age up to eleven week. After that, the curvature of the fetus affects the reliability of the measurement. From the twelfth week onwards, the biparietal diameter is more accurate. Using scans in different directions, the longest length of the embryo should be found and a measurement made from the head (cephalic pole) to the outer edge of the rump (Figure 2.33). The yolk sac should not be included (Breyer et al, 1993).

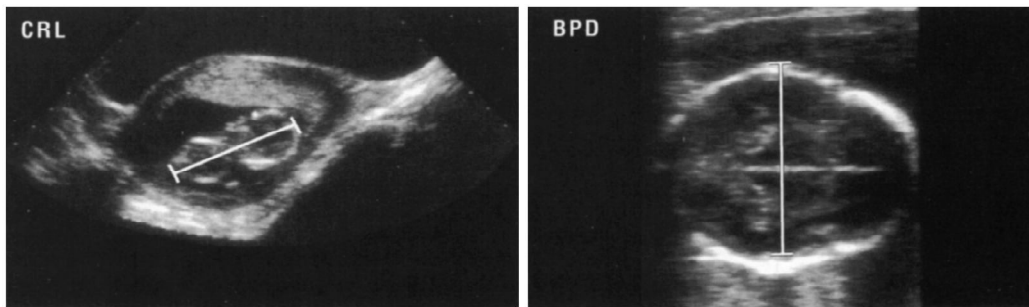


Figure (2.33) ultrasound image shows up to 11 weeks (left) measure the crown-rump length after 11 weeks (right) measure the biparietal diameter (Breyer et al, 1993).

2-5-2 Biparietal diameter:

This is the most reliable method of estimating gestational age between the 12th and the 26th weeks. After that, its accuracy may be lessened by pathological disorders and biological variations that affect fetal growth. It must be considered together with other measurements, such as femoral length and abdominal circumference. The biparietal diameter (BPD) is the distance between the parietal eminences on either side of the skull and is, therefore, the widest diameter of the skull from side to side. Using scans at different angle, the transverse section will be recognized when the shape of the fetal skull is ovoid and the midline echo from the falx cerebri is interrupted by the cavum septi pellucid and the thalami. When this plane is found, the gain on the ultrasound unit should be reduced and measurements

made from the outer table of proximal skull (the part nearest to the transducer) to the inner table of the distal skull (the part farthest away from the transducer). The soft tissues over the skull are not included (Breyer et al, 1993).

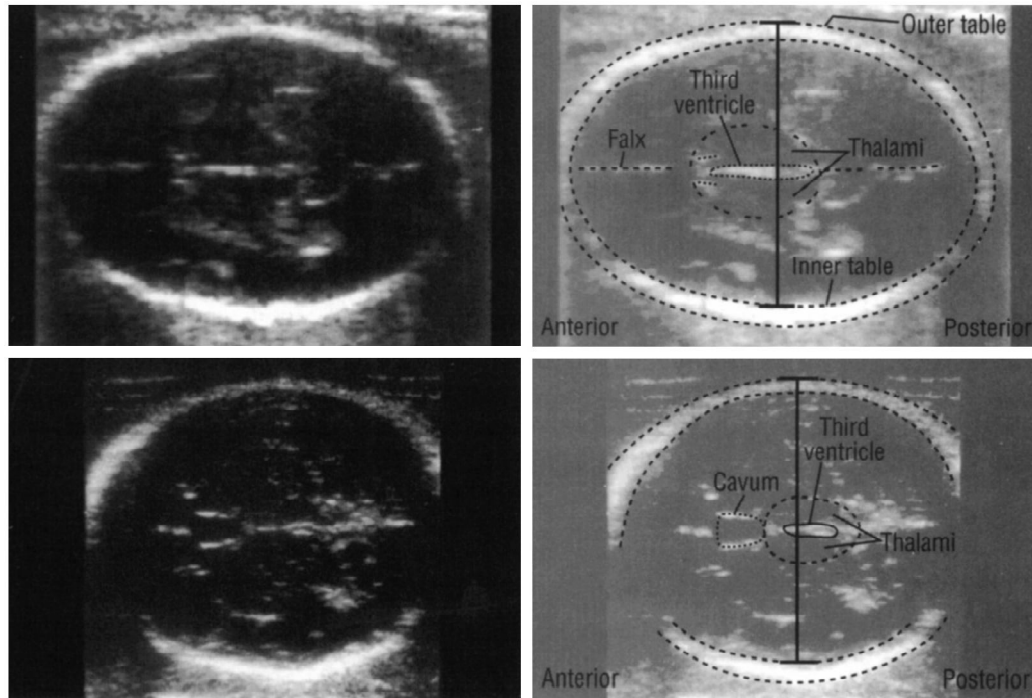


Figure (2.34)ultrasound image shows the fetal skull at 24 weeks' gestation, scanned at two different levels. The biparietal diameter is the widest distance from the outer edge of the proximal skull to the inner edge of the distal skull. At the correct level the midline falx is interrupted by the cavum septi-pellucidum(Breyer et al, 1993)

Problems that affecting accuracy of BPD are incorrect angle, If the angle of the probe on the maternal abdomen is incorrect, the midline echo does not lie centrally within the fetal skull. Similarly, the echoes from the lateral ventricles will not be visualized symmetrically about the midline. The angle of the probe to the maternal abdomen should be altered, without sliding or rotating the probe; incorrect rotation which is readily recognized because the visualized shape of the fetal skull is usually too round –and/or not all the landmark features are seen. Rotating the probe will correct the shape but

you must be careful to maintain the correct angle; incorrect level, sliding movements of the probe will alter the level of section. Be careful not to rotate or change the angle of the probe as you slide; midline not horizontal because having obtained the correct section displaying the required landmarks check that the midline is not lying at an angle to the horizontal. Dipping one end of the probe will orientate the head into the correct position; BPD measurements in breech and transverse presentations which can be unreliable in the second half of pregnancy. In these presentations the fetal head might be dolichocephalic (long and narrow) in shape. This produces a BPD measurement that is artifactually small for gestational age. The head circumference measurement, however, is unaltered by presentation and is therefore a reliable indicator of gestational age irrespective of fetal presentation, and OP/OA position, measurement of the BPD should only be taken when the fetal head is in the occipitotransverse (OT) position, because the landmarks are best recognized when the midline echo and the other landmarks are at 90° to the ultrasound beam. The BPD should therefore not be measured if the fetal head is directly occipitoposterior (OP), directly occipitoanterior (OA) or deep in the maternal pelvis. Tilting the woman into a 45° head-down position and/or partially flexing the fetal head such that it can be measured. (Chudleigh and Thilaganathan, 2004).

2-5-3 Fronto-occipital diameter:

The fronto-occipital diameter is measured along the longest axis of the skull at the level of the biparietal diameter (BPD). From outer edge to outer edge (Breyer et al, 1995).

2-5-4 Cephalic –index:

The BPD is a reliable estimate of gestational age except when the shape of the head is an abnormality of the intracranial content. The adequacy of the

head shape is determined by comparing its short axis to its long axis (Breyer et al, 1995).

2-5-5 Head circumference (HC):

Head circumference (HC) is taken at the level of BPD and can be calculated from the same frozen image. Most modern ultrasound equipment has built-in electronic calipers that open to the outline of the fetal head. To obtain an accurate HC measurement, 60% to 70% of the skull outline should be displayed on the screen (Hagen-Ansert, 2001).

2-5-6 Abdominal circumference (AC):

Obtain a longitudinal view of the fetus that demonstrates both the fetal heart and the fetal bladder. Slide the transducer laterally until the fetal spine is visualized. Rotate the transducer through 90° at the level of the fetal stomach to obtain a cross-section.(Figure 2.35) illustrates the section on which the AC is measured. The landmark features are a circular section of the abdomen demonstrating an unbroken and short rib echo of equal size on each side; a cross-section of one vertebra visualized as a triangle of three white spots; a short length of umbilical vein, and the stomach, usually visualized as a hypoechoic area in the left side of the abdomen (Chudleigh and Thilaganathan, 2004).

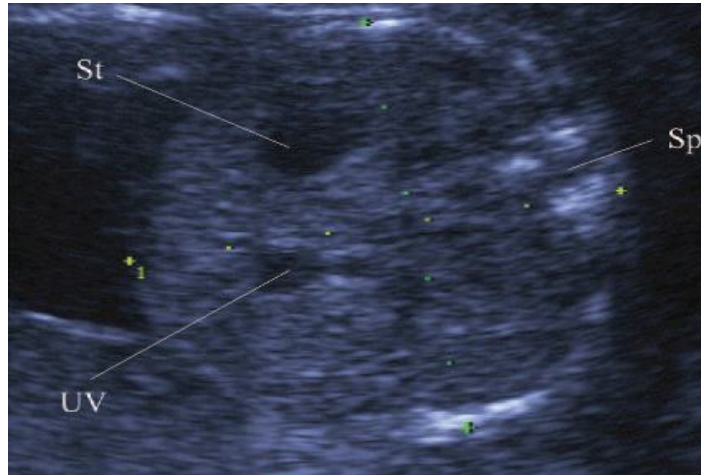


Figure (2.35) ultrasound image shows Transverse section of the fetal abdomen demonstrating the landmarks required to measure the abdominal circumference. Note the appearance of the normal single vertebra (Sp), the short length of umbilical vein (UV) and its position. Note also the appearance and position of the normally sized stomach (St)

(Chudleigh and Thilaganathan, 2004).

The AC can be measured with the same instruments used to measure the HC. The calipers should be placed along the external perimeter of the fetal abdomen to include subcutaneous soft tissue (Hagen-Ansert, 2001).

Problems that affecting the accuracy of AC are directly anterior fetal spine, the umbilical vein will not be seen in transverse section because it lies in the acoustic shadow produced the transducer to a more lateral position on the maternal abdomen, or to dip one end of the transducer, to allow the umbilical vein to be imaged; long length of umbilical vein, The umbilical vein travels up through the liver at approximately 45° . Thus, if the section on which you intend to measure the AC demonstrates a long length of umbilical vein, you know you have an oblique and incorrect section. If the longitudinal fetal spine is in the horizontal plane then angling is required, if the longitudinal fetal spine is at an angle to the horizontal then rotation is required ; non-circular outline, an oval outline indicates an oblique cross-section. This can be rectified by a slight change in rotation or angle – the choice depends on

the position of the fetal body relative to the horizontal plane. If the longitudinal fetal spine is in the horizontal plane then rotation is required, if the longitudinal fetal spine is at an angle to the horizontal then angling is required (Chudleigh and Thilaganathan, 2004).

The AC may change shape with fetal breathing activity, transducer compression, or intrauterine crowding(as in multiple pregnancies or oligohydramnios) or secondary to fetal position, as in a breech presentation (Hagen-Ansert, 2001).

2-5-7 Fetal long bone measurements:

When measuring bone length, it is necessary to reduce the gain. It is usually easy to see fetal long bones from 13 weeks onwards (Breyer et al, 1995).

2-5-7-1 Femur length (FL):

The most widely measured and easily obtainable of all fetal long bones is the femur. FL is about as accurate as BPD in determining gestational age. Femur length is an especially useful parameter that can be used to date a pregnancy when a fetal head cannot be measured because of position or when there is a fetal head anomaly (Hagen-Ansert, 2001).

Measuring the femur is ideally undertaken after the AC has been measured. Slide the probe caudally from the AC section until the iliac bones are visualized. At this point, a cross-section of one or both femurs is usually seen. The upper femur should be selected for measurement. The lower femur is frequently difficult to image clearly because of acoustic shadowing from fetal structures anterior to it. Keeping the echo from the anterior femur in view, rotate the probe slowly until the full length of the femur is obtained (Chudleigh and Thilaganathan, 2004).

Hyperechoic linear structure represents the ossified portion of the femoral diaphysis and corresponds to femoral length measurement from the greater trochanter to the femoral condyles. These are imaged as rounded

hypoechoic masses at each end of the diaphysis called the epiphyseal cartilages; they should not be included in the femoral length measurement (Figure 2.36) (Hagen-ansert, 2001).

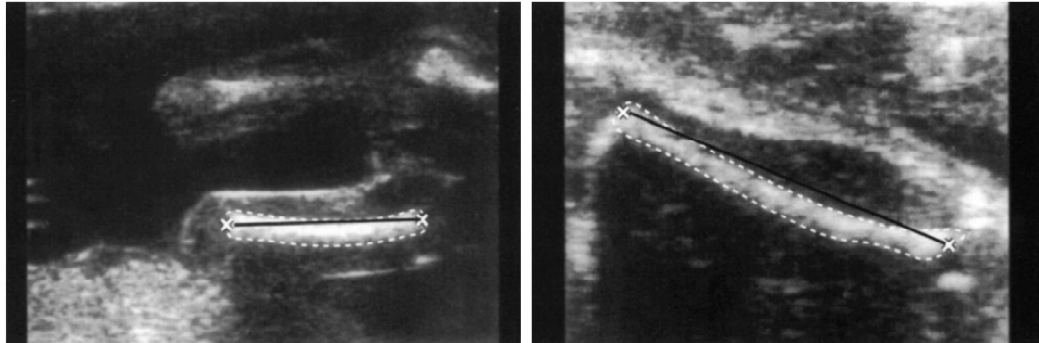


Figure (2.36) ultrasound image shows the length of the femur is measured from end to end. In older fetuses (right), there is an ossification centre at the distal end of the femur; this is not included in the measurement (Breyer et al, 1995).

Overestimating the length of the femur by high gain settings or by including the femur head or distal epiphysis in the measurement is possible. Underestimation can result from using incorrect plane orientation and not obtaining the full length of the bone (Hagen-Ansert, 2001).

Most problems arising with measuring the FL are due to a combination of fetal movements and slow use of the freeze button. If the end-points of the femur cannot be adequately visualized, unfreeze the image and seek another, better image also one or both end-points are difficult to define then dip one end of the probe gently in to the maternal abdomen. The upper femur appears straight but the lower femur appears bowed The slight bowing seen in the lower limb is a normal artifact of the imaging process. Unilateral femoral abnormalities are very rare but should always be considered as a possible, if unlikely, explanation for significant dissimilarity in the appearance of the two femurs. An experienced second opinion should be sought if necessary (Chudleigh and Thilaganathan, 2004).

In any routine obstetric evaluation, the femur is usually the only long bone measured, but if there is a 2-week or longer difference between femur length and all the other biometric parameters, all fetal long bones should be measured and a targeted examination of the fetal anatomy should be performed (Hagen-Ansert, 2001).

2-5-7-2 Tibia and Fibula:

The tibia and fibula can be measured by first identifying the femur, then following it down until the two parallel bones can be identified. The tibia can be identified because the tibial plateau is larger than the fine tapering fibula. The tibia is located medial to the fibula. Measure length point to point(Figure2.37)(Hagen-Ansert, 2001).

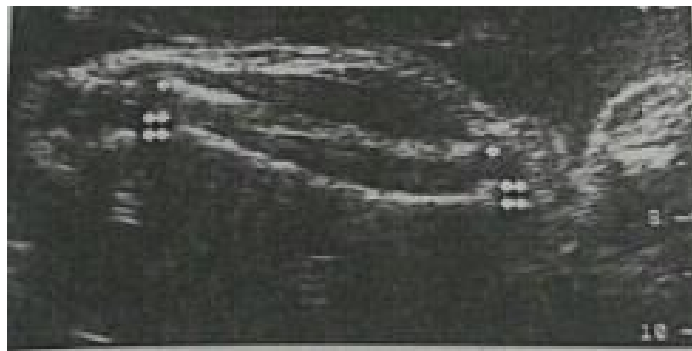


Figure (2.37)ultrasound image shows the tibia and fibula. The tibia can be distinguished from the fibula because the tibia is larger (multiple arrows) than the small tapering fibula (single arrow) (Hagen-Ansert, 2001).

2-5-7-3 Humerus:

Humerus length is sometimes more difficult to measure than femur length. The "up side" humerus, falls in the near-field zone, where detail is not always focused and the acoustic shadow is less clear. The opposite, or "down side" humerus may be obscured because of overlying fetal spine or fetal ribs. Image fetal spine in upper thoracic-lower cervical region. Identify scapula, then rotate transducer until long axis of humerus is seen. Only humeral shaft

(diaphysis) is ossified and should be measured (figure 2-38) (Hagen-Ansert, 2001).



Figure (2.38) ultrasound image shows longitudinal section through a fetal humerus. The calipers should be placed at the most distal ends of the bone (Hagen-Ansert, 2001).

2-5-7-4 Radius and Ulna:

The radius and ulna can be recognized by following the humerus down until two parallel bones are visualized and then rotating the transducer slightly until the full length of the bones is identified. The ulna can be distinguished from the radius because it penetrates much deeper into the elbow (Fig2-39). The ulna is larger and anatomically medial (Hagen-Ansert, 2001).

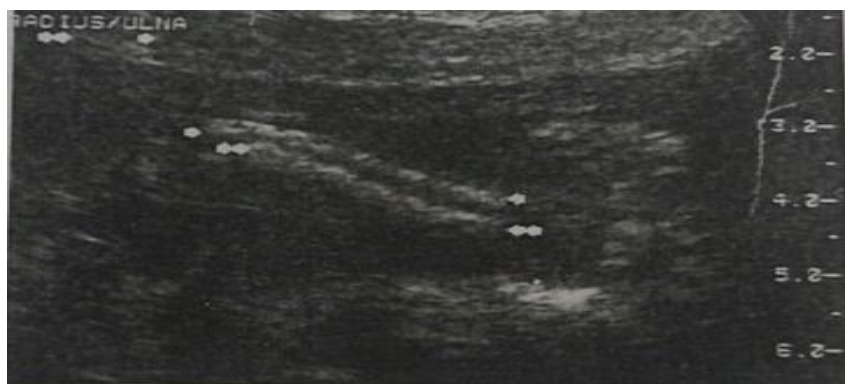


Figure (2.39) ultrasound image shows a longitudinal section through the radius (two arrows) and ulna (one arrow) at 20.3 weeks of gestation. The calipers should be placed at the most distal portion of each individual bone (Hagen-Ansert, 2001).

There are many problems in obtaining accurate measurements of limb bones and in evaluating their growth. The limb length measurement may be affected by several factors; both the angle of the beam to the long axis of the bone and the type of transducer (linear vs. curvilinear vs. sector) can change the amount of artifactual echoes at the extremities of the bones. Also, there is the factor of the level of experience of the operator, which can be assessed by differences of intraobserver variation (Lessoway et al, 1990).

No single parameter is perfect in predicting gestational age. Use of multiple parameters in estimating fetal age is appropriate only when the fetus is growing normally. The value of using multiple parameters is that although any of the measurements may be technically incorrect, it is unlikely that all of the measurements are overestimated or underestimated (Hagen-Ansert, 2001).

2.6 Previous studies:

Exacoustos, et al 1991 had done study about ultrasound measurements of fetal limb bones to establish the growth patterns of fetal limbs, measurement of femur, humerus, tibia, fibula, radius and ulna that made by ultrasound and related to gestational age. To this end, 2317 normal singleton pregnant women were studied cross-sectionally at 13-40 weeks of gestation. Patients were selected on the basis of a certain last menstrual period, history of regular cycles and at least one ultrasound scan before 16 weeks confirming gestational age. The ultrasound examinations were performed with General Electric RT 36000 (Milwaukee, Wisc.). The result shows a rapid increase in limb bone growth from 15 to 28 weeks, followed by a decrease in the weekly increment. The measurements of all six fetal long bones showed a high correlation with menstrual age ($r \geq 0.99$). Femur length ($r = 0.994$; $p < 0.0001$), humerus length ($r = 0.993$; $p < 0.0001$), tibia length ($r = 0.994$; $p < 0.0001$), fibula length ($r = 0.994$; $p < 0.0001$), radius length ($r = 0.988$; $p < 0.0001$), ulna length ($r = 0.993$; $p < 0.0001$).

Chitty and Altman, 2002 they were done study about Chart of fetal size: limb bones to construct new size charts for all fetal limb bones. 663 fetuses scanned once only for the purpose of the study in the ultrasound department of King's College Hospital at gestations between 12 and 42 weeks. All long bones (radius, ulna, humerus, tibia, fibula and femur) were measured in a plane such that the bone was as close as possible to a right angle to the ultrasound beam. The radius and ulna, tibia and fibula were measured independently and shows the increasing variability of the measurements with increasing gestational age. The growth of the upper limbs accelerated compared with the lower limbs.

Queenan JT et al, 1980 had done study about ultrasound measurement of fetal limb bones. A study was made of 41 patient with known menstrual dates in whom the duration of gestation, as determined physical examination and

ultrasound scan, corresponded with those dates. Examination of the fetal limb lengths was done every 1 to 3 weeks starting at 8 weeks' gestation. Akretzcombison 100 ultrasound sector scanner with a 2.5MHz transducer was used. Serial measurements of the humerus, femur, radius-ulna, and tibia-fibula complexes were made. The growth rate of fetal limb bones was linear from 12 through 22 weeks' gestation but the various bones appeared to grow at different rates. All of limb bone lengths correlate with gestational age.

Chapter Three

Material and Methods

3- 1 Type of the study:

This is descriptive cross-sectional study

3-2 The material:

The study was involved one hundred and forty cases of Sudanese singleton pregnant ladies (each twenty pregnant women at 14, 18, 22, 26, 30, 34, 38 weeks of gestational age) who were came routinely for assessment of gestational age to ultrasound department of Oma-algora specialize hospital, Aljazeera-Sudan during the period from July 2016 to February 2017.

3.2.1 Inclusion criteria:

Normal singleton pregnant women who were informed consent to participate in the study.

3.2.2 Exclusion criteria:

Maternal disease or medication which was likely to affect the growth of the fetus (diabetes mellitus, renal disease, hypertension requiring treatment, etc), Multiple pregnancy, fetuses diagnosed to have congenital anomalies prenatally, placental and liquor abnormalities, Intrauterine fetal growth retardation.

3.2.3 Study variables:

Gestational age, fetal radius, ulna, fibula and tibia.

3-3 Methods:

3-3-1 Equipment for data collection:

LOGIQ 100 PRO (portable digital ultrasound system) power 170 VA, manufactured on Japan 2001, with 3.5MHz convex-Array probe, 50 mm radius, 68° field of view.

3-3-2 Tools of data collection:

The data was collected by data collection sheets and ultrasound findings.

3-3-3 Scanning technique:

Sonographic examination was obtained for all participants (140 pregnant ladies) in supine position using 3.5 MHz convex transducer with a coupling gel which was applied to ensure good acoustic contact between the transducer and skin and allow optimum transmission of the sound beam. Women were selected on the basis of certain last menstrual period, history of regular cycle. Fetal head was identified to determine presentation of the fetus and then heart was located to confirm viability. A general survey of the fetus was done to rule out any anomalies. Liquor quantity was assessed. Placental location and maturity was noted.. The fetal gestational age was calculated by using BPD, HC, AC and FL measurements in weeks.

3-3-3-1 Scanning technique for ulna and radius:

To locate ulna and radius firstly identify the humerus so slide the transducer until the fetal heart is identified with in the fetal chest and scanning through fetal ribs/thorax and shoulder girdle leading to the adjacent humerus. By tracing the humerus to the elbow, the ulna and radius are imaged in transverse sections, two bones which are seen as echogenic dots. Then, with a probe rotation of 90 degrees, a sagittal plane is obtained and the long axis of each bones is identified. The radius and ulna can be well differentiated and measured when the arm is in a supine position because the two bones are lying exactly parallel. In prone position the crossing of two bones requires two different ultrasonic planes to obtain measurements. Measured radius and ulna separately by placing ultrasound calipers on two points at either end of each bone, the length were measured in cms, three or more measurements are taken in each examination to obtain the accurate mean measurement. Care was taken to ensure that the full length of the bone was visualized.

3-3-3-2 Scanning technique for tibia and fibula:

To locate fetal tibia and fibula firstly identify the femur, by moving the transducer transversely across the abdomen till iliac bones and bladder were seen. Then, turning the probe sagittaly, the long femur bone was identified. After that moving the transducer inferior to the femur until two echogenic dots comes into view (transverse section), then rotate the probe until the long axis of two parallel bones can be identified. By placing the ultrasound cursers on both ends of the each bones, the length was measured in cms, three or more measurements were taken in each examination to obtain accurate measurement. The bones were measured in aplane such that the bone was as close as possible to a right angle to the ultrasound beam.

3-3-4 Interpretation:

done by sonologist

3-3-5 The method of data analysis used in the study:

The data collected in master data sheet was analyzed by using excel and statistical package for social sciences (SPSS) version 20 for windows (IBM, USA). The tables are used in the analysis and caried out the relationship between different variables was presented by using tables and graphs.

Chapter four

The Results

4-1 The results:

Table (4-1) shows mean, standard deviation, minimum, and maximum length of radius in different gestational age.

Gestational Age		N	Mean	Std. Deviation	Minimum	Maximum
Radius	14 Weeks	20	1.0360	.03817	1.00	1.11
	18 Weeks	20	2.0610	.08540	1.85	2.20
	22 Weeks	20	3.1380	.04561	3.10	3.25
	26 Weeks	20	4.0220	.16551	3.55	4.12
	30 Weeks	20	4.4920	.12923	4.30	4.65
	34 Weeks	20	4.8130	.13581	4.67	5.18
	38 Weeks	20	5.4910	.19210	5.22	5.93
Total		140	3.5790	1.48308	1.00	5.93

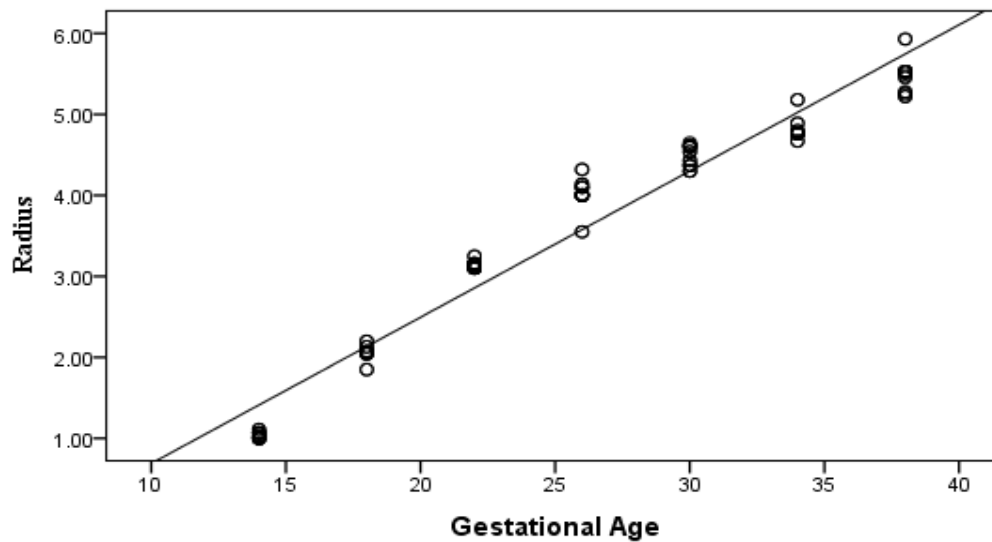


Figure (4-1): scatter plot diagram shows the positive linear relation between gestational age by weeks in the X axis and measured RL by cm in Y axis.

Table (4-2) shows mean, standard deviation, minimum, and maximum length of ulna in different gestational age.

GestationalAge		N	Mean	Std. Deviation	Minimum	Maximum
Ulna	14 Weeks	20	1.2260	.04358	1.15	1.31
	18 Weeks	20	2.2600	.08547	2.05	2.40
	22 Weeks	20	3.3580	.05483	3.30	3.45
	26 Weeks	20	4.3340	.44346	3.75	4.54
	30 Weeks	20	4.9905	.18326	4.71	5.28
	34 Weeks	20	5.5680	.05483	5.50	5.66
	38 Weeks	20	6.3190	.33395	6.15	6.53
Total		140	4.0079	1.71337	1.15	6.53

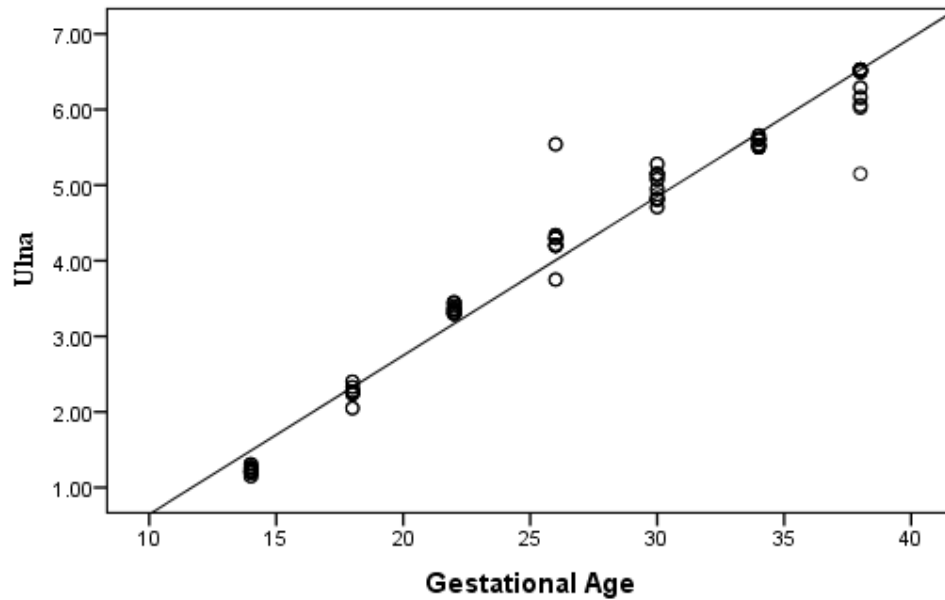


Figure (4-2): scatter plot diagram shows the positive linear relation between gestational age by weeks in the X axis and measured UL by cm in Y axis.

Table (4-3) shows mean, standard deviation, minimum, and maximum length of fibula in different gestational age.

GestationalAge		N	Mean	Std. Deviation	Minimum	Maximum
Fibula	14 Weeks	20	1.1210	.07100	1.04	
	18 Weeks	20	2.1310	.08577	1.97	2.30
	22 Weeks	20	3.2700	.08932	3.20	3.44
	26 Weeks	20	4.2120	.12138	4.02	4.52
	30 Weeks	20	4.8900	.16815	4.59	5.11
	34 Weeks	20	5.5160	.07950	5.35	5.64
	38 Weeks	20	6.0715	.59034	5.81	6.48
Total		140	3.8874	1.69848	1.04	6.48



Figure (4-3): scatter plot diagram shows the positive linear relation between gestational age by weeks in the X axis and measured FiL by cm in Y axis.

Table (4-4) showing mean, standard deviation, minimum, and maximum length of tibia in different gestational age.

Gestational age		N	Mean	Std. Deviation	Minimum	Maximum
Tibia	14 Weeks	20	1.2950	.05790	1.15	1.38
	18 Weeks	20	2.3310	.08577	2.17	2.50
	22 Weeks	20	3.4600	.07455	3.40	3.64
	26 Weeks	20	4.3120	.33779	3.39	4.72
	30 Weeks	20	5.0955	.16732	4.79	5.31
	34 Weeks	20	5.7170	.08027	5.55	5.84
	38 Weeks	20	6.4755	.23189	6.04	6.68
Total		140	4.0980	1.73447	1.15	6.68

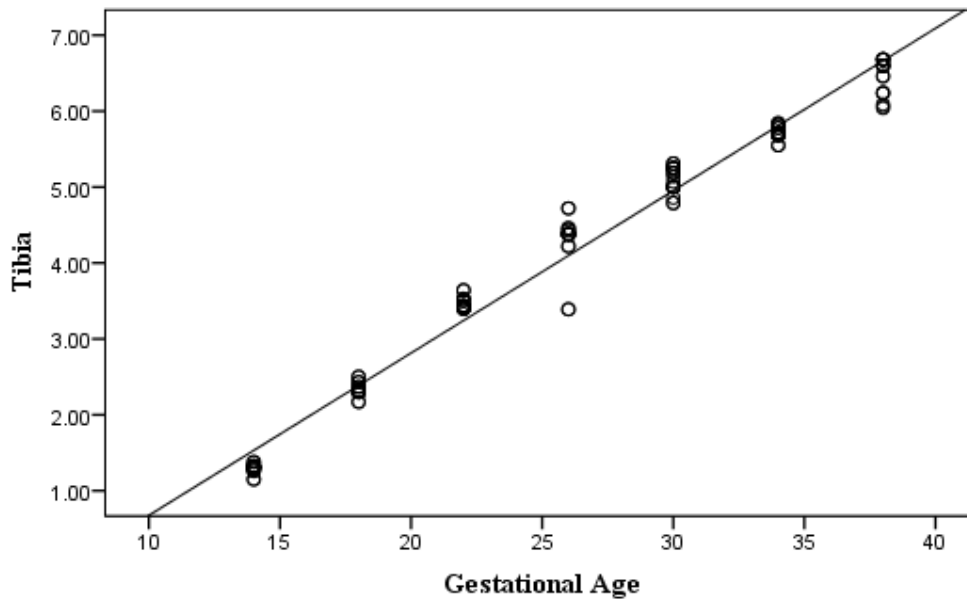


Figure (4-4): scatter graph shows the positive linear relation between gestational age by weeks in the X axis and measured TL by cm in Y axis.

Table(4-5) shows the correlation between the Gestational Age and measurement of RL, UL, FiL,TL.

		Gestational Age
Radius	Pearson Correlation	0.977**
	Sig. (2-tailed)	0.000
Ulna	Pearson Correlation	0.984**
	Sig. (2-tailed)	0.000
Fibula	Pearson Correlation	0.981**
	Sig. (2-tailed)	0.000
Tibia	Pearson Correlation	0.990**
	Sig. (2-tailed)	0.000

Key (**. High Correlation. Significant less than 0.05 .)

The equations are:

$$\text{Gestational Age} = 5.29 * \text{Radius Length} + 7.06$$

$$\text{Gestational Age} = 4.61 * \text{Ulna Length} + 7.51$$

$$\text{Gestational Age} = 4.63 * \text{Fibula Length} + 7.96$$

$$\text{Gestational Age} = 4.58 * \text{Tibia Length} + 7.22$$

Chapter five

Discussion, Conclusion and Recommendation

5-1 Discussion:

This is a descriptive cross sectional study aimed to measure fetal radius, ulna, fibula, and tibia by ultrasound at 14-38 weeks of gestation and related them to gestational age. This study conducted in 140 normal singleton pregnant sudanese women (each twenty pregnant women at 14,18, 22, 26, 30, 34, and 38 weeks of gestational age) who were came to the area of the study.

On this study descriptive statistic such as mean \pm SD, minimum, and maximum shows the symmetry of data distribution and the validity of the assumption of normality see table (4-1), (4-2), (4-3), (4-4).

The study shows that the growth of the fetal radius, ulna, fibula and tibia was linear from 14 through 38 weeks' gestation, but the various bones appeared to grow at different rates figures (4-1), (4-2), (4-3), (4-4) which is agree with the result of (QueenanJT et al, 1980) . It is difficult to explain the differences observed in growth rates among long bone measurements. Since all bones are subjected to similar intra-uterine enviromental factors. It also revealed that growth pattern of long bone length, early fetal development is characterized by accelerated growth of these bones from 14 to 30 weeks followed by a decrease in weekly increment rate, this agree with (Exacoustos et al, 1991) but the acceleration from 15 to 28 weeks and this may be due to large sample. Furthermore the growth of the radius and ulna accelerated compared with the fibula and tibia; this result was in line with previous study (Chitty and Altman, 2002).

This study revealed that there was strong correlation between gestational age in weeks and RL, UL, FiL and TL in cm ($r=0.997$), ($r=0.984$), ($r=0.981$) and ($r=0.990$) respectively. The paired 2- tailed (t-test) between GA/weeks and measurement of RL/cm, UL/cm, FiL/cm, and TL/cm shows that the result

was statistically significant ($P=0.000$) see table (4-5) which is agree with the result of (QueenanJT et al, 1980) and (Exacoustos et al, 1991) because it shows a high correlation between gestational age by weeks and measurements by mm of RL($r=0.988$; $P<0.0001$), UL($r=0.993$; $P<0.0001$), FiL($r=0.994$; $P<0.0001$), and TL($r=0.994$; $P<0.0001$).

The equations are:

$$\text{Gestational Age} = 5.29 * \text{Radius Length} + 7.06$$

$$\text{Gestational Age} = 4.61 * \text{Ulna Length} + 7.51$$

$$\text{Gestational Age} = 4.63 * \text{Fibula Length} + 7.96$$

$$\text{Gestational Age} = 4.58 * \text{Tibia Length} + 7.22.$$

5-2 conclusion:

1. This study found significant correlation between gestational age (GA) and lengths of radius, ulna, fibula, and tibia, that can be used in the assessing of gestational age as additional parameter and in monitoring fetal growth and for diagnosing of bone dysplasia.
2. This study also found linear relation between GA by weeks and measurements of radius, ulna, fibula, and tibia lengths by cm.
3. This study found that the accuracy of measurement of these bones before the 14th is too poor for use in dating pregnancies so we begin the study from this week.

5.3 Recommendations:

1. Study recommended that the modern ultrasound machines and increase the training institutes of ultrasound for increasing the sonologists skills and experiences should be advisable.
2. Increasing the number of the specialist hospitals for obstetric and gynaecology diseases because they increased in Sudanese now days.
3. Finding a reference value for Sudanese fetal radius, ulna, fibula and tibia can be obtained if such issue is targeted by comprehensive studies and compare them with other modalities.
4. Further study to show if maternal nutrition and tribes had effect on RL, UL, FiL and TL or not.

References:

- Bar-Harval, Bronshtein M, Orvieto R, et al. Caution: prenatal clubfoot can both transient and a late-onset phenomenon. *Prenatal Diagn.* 1997; 17(5): 457-60 [pubmed].
- Benacerraf BR. Antenatal sonographic diagnosis of congenital clubfoot: a possible indication for amniocentesis. *J Clin ultrasound.* 1986; 14(9): 703-6. [pubmed].
- Breyer, B., Bruguera C.A., Ghabi, H.A., Goldberg, B.B., Tan, F.E.H., Wachira, M.W. and Weill, F.S. 1995. *Manual Diagnostic ultrasound.* Geneva: World Health Organization. P 3, 12, 20, 236-238, 240.
- Bronshtein M, Zimmer EZ. Transvaginal ultrasound diagnosis of fetal clubfeet at 13 weeks, menstrual age. *J Clin ultrasound.* 1989; 17(7):518-20 [pubmed].
- Chitty, L. S. & ALTMAN, D. G. 2002. Charts of fetal size: limb bones. *BJOG*, 109, 919-29.
- Chudleigh, T. and Thilaganathan, B. , 2004. *Obstetric ultrasound how, why and when*, 3rd edition, Elsevier, Churchill Livingstone. P 17-18, 20-23, 30-33, 95, 97, 101, 105-108.
- Duijf PH, VanBokhoven H, Brunner HG. Pathogenesis of split-hand/split-foot malformation. *Hum Mol Genet.* 2003;12 (spec No1): R51-60 [pubmed].
- Elliott AM, Evans JA, Chudleg AE. Split hand foot malformation (SHFM) *Clin Genet.* 2005; 68(6):501-5.[pubmed].
- Emanuel PG, Garcia GI, Angtuaco TL. Prenatal detection of anterior abdominal defects with US. *Radiographics.* 1995;15(3): 517-30 [pubmed].
- Espinasse M, Manouvriers, Boute O, et al.[embryofetopathy only little Known. Apropos of 4 cases] *Arch pediatr.* 1996;3(9):896-9. [french] [pubmed].
- Exacoustos C, Rosati P, Rizzo G, et al. Ultrasound measurement of fetal limb bones. *Ultrasound Obst Gynaecol* 1991;1(5):325-330. [Jebmh.com].

Granellini D, Fieni S, Vadora E. Prenatal diagnosis of isolated limb defects: an updated review. *Fetal diagnosis and therapy*. 2005;20(2):96-101.[pubmed].

Hagen-Ansert, S.L. 2001. Textbook of diagnostic ultrasonography, volume 2, 5th edition. United States of America: Mosby, Inc.. P 590, 625, 668-671, 775-776, 778, 780, 783-784,792-793, 871, 875-877, 918-925, 927-929, 931, 970.

Issel, E.P.(1985). Ultrasonic measurement of the growth of fetal limb bones in normal pregnancy. *J. perinat. Med.*,13, 305-13.

Jain A, Kumar G,Aganwal U, et al. Placental thickness- asonographic indicator of gestational age. *J of obst and Gyne of india*. 2001;51(3):48-9. [www.ijmrp.com].

Jeanty P, RodeschF, Delbeke D et al. Estimation of gestational age from measurements of fetal long bones. *J Ultrasound Med* 1984; 3(2): 75-79.

Jeanty, P., Dramaix-Wilmet, M., van Kerkem, J., petroons, P.andSchwers, J. (1982). Ultrasonic evaluation of fetal limb growth. 11. *Radiology*, 143, 751-4.

Jeffrey S Robinson. Fetal growth and development In: Geoffrey Chamberlain, Ed. *Turnbell's Obstetrics*, 2nd edition. HongKong, Churchill Livingstone, 1995, 97-114 [www.ijmrp.com].

Johnson J-AM. In: Rumack CM, Wilson SR,Charboneau JW, editors. *Diagnostic Ultrasound*. 3rd edition. St. louis, Mo. Elsevier; 2005. Overview of obstetric sonography. p. 1039-58.

Krebs, C.A., Giyanani, V.L. and Eisenberg, R.L. 1993. *Ultrasound Atlas Of Disease Processes*, Appleton & lange, Norwalk, Connecticut. P 1, 2, 3.

Kurjak, A and Chervenak, F.A., 2003. *Donald School Textbook of Ultrasound in Obstetrics and Gynecology*. NewDelhi: Parthenon publishing. P 74, 178-179.

Lamb DW, Wynne-Davies R, soto L. An estimate of the population frequency of congenital malformations of the upper limb. *J Hand Surg [Am]* 1982; 7(6): 557-62.[pubmed].

Lazebnik, N. and Lazebnik, R.S. 2008. *Advanced Obstetrical Ultrasound.*, Elsevier Inc. P 2, 565, 567-568, 600-601.

LEE, W., BALASUBRAMANIAM, M., DETER, R. L., HASSAN, S. S., GOTSCH, F., KUSANOVIC, J. P., GONCALVES, L. F. & ROMERO, R. 2009. Fetal growth parameters and birth weight: their relationship to neonatal body composition. *Ultrasound Obstetric & Gynaecology*, 99, 626-627.

Lessoway, V., Schulzer, M and Wittmann, B.K. (1990). Sonographic measurement of fetal femur: factors affecting accuracy. *J. Clin. Ultrasound*, 18, 471- 6.

Light TR. In: peimer CA, editor. *Surgery of the hand and upper extremity.* New York: McGraw-Hill; 1996. Congenital anomalies: syndactyly, polydactyly and cleft hand. Pp. 2111-44.

Merz, E., Kim-Kern, vM. S. and Pehl, S. (1987). Ultrasonic measurement of fetal limb bones in the second and third trimesters. *J. Clin. Ultrasound*, 15, 175-83.

Romero R, Athanassiadis AP, Jeanty P. Fetal skeletal anomalies. *Radio L clin North Am.* 1990;28 (1):75-99.[pubmed].

Salder, T.W., Langman's medical embryology, 13th edition. London: Wolters Kluwer Health. 2015; p 47-48, 56-57, 92-94, 103-104, 105-106, 125, 163, 165, 174.

Stollc, Finck S, Janser B, et al. Tau syndrome (thrombocytopenia and absent ulnar) with maternal retardation and facial dysmorphism. *Genet Couns.* 1992; 3 (1): 41-6 [pubmed].

Taybi H, Lachman R. *Radiology of syndromes, metabolic disorders and skeletal dysplasias.* 5th edition. St. Louis, Mo: Mosby. 1996.

Teot L, Deschamps F. [Histologic and echographic correlations of the hip in newborn infants] Rev chir orthop Reparatrice Appar Mot. 1990; 76 (1):8-16 [French] [pubmed].